Available online at www.sciencedirect.com
ScienceDirect
Computers and Structures 86 (2008) 47–63
Computers & Structures
www.elsevier.com/locate/compstruc

A nonlinear beam element formulation in the framework of an energy preserving time integration scheme for constrained multibody systems dynamics

Elisabet V. Lens, Alberto Cardona *

Centro Internacional de Métodos Computacionales en Ingeniería, CIMEC-INTEC, Conicet-Universidad Nacional del Litoral, Güemes 3450, 3000 Santa Fe, Argentina

Received 5 September 2006; accepted 15 May 2007
Available online 17 July 2007

Abstract

A nonlinear large rotations beam element is presented within the framework of an energy conserving algorithm which was presented in previous works [Lens E, Cardona A, Géradin M. Energy preserving time integration for constrained multibody systems. Multibody System Dyn 2004;11:41–61; Lens E. Energy preserving/decaying time integration schemes for multibody systems dynamics. PhD thesis, Universidad Nacional del Litoral, Argentina; 2006]. Flexibility is dealt with easily in energy conserving algorithms only for finite element models with displacement degrees of freedom. However, beam models which have rotation degrees of freedom are more cumbersome to be handled. The beam model which we introduce in this paper has simplifications that lead to quite compact expressions of its different terms. This kind of algorithms has many advantages, both theoretical and practical, because of its unconditional stability which is guaranteed even in the nonlinear regime.

Keywords: Flexible multibody dynamics; Nonlinear beam; Energy conservation; Large finite rotations; Flexible dynamics impacts

1. Introduction

Although the physical theory of beams undergoing large rotations is widely known from long time (see for instance [3–6]), the development of algorithms to simulate the time response of beams is in continuous evolution.

The computation of the response of beams requires the use of a time integration strategy that deserves particular attention. The numerical solution of the equations of motion of the system may give rise to difficulties of purely numerical origin which come out in the form of instabilities of the solution or in the form of high frequency oscillations. Time integration schemes that preserve the total energy of the system guarantees at least the answer to the instabilities, as it was shown by Hughes [7].

Different energy preserving beam models have been proposed in the bibliography. Bauchau [8] proposed a beam model that consists of a geometrically exact, shear deformable beam undergoing arbitrary large displacements and rotations but small strains. On the other hand, the model of Ibrahimbegovic et al. [9] essentially represents a convenient reparameterization of the classical beam model of Love [10] and Reissner [3], proposed initially by Simo [5] for straight beams, reworked by Cardona and Géradin for multibody dynamics applications [6] and extended by Ibrahimbegovic [11] to space curved beams. Romero and Armero [12] proposed a finite element implementation of the model presented by Simo [5] that corrects the lack of objectivity due to the adopted spatial finite element interpolations. Bottasso et al. [13–17] developed a novel approach for the integration of general nonlinear multibody dynamics problems that includes geometrically exact beams, where schemes with preservation and dissipation of

* Corresponding author.
E-mail address: acardona@intec.unl.edu.ar (A. Cardona).

0045-7949/$ - see front matter © 2007 Elsevier Ltd. All rights reserved.
doi:10.1016/j.compstruc.2007.05.036

the energy are devised. More recently, Leyendecker et al. [18] introduced modifications in the beam formulation of Betsch and Steinmann [19,20] to obtain a time-stepping scheme energy–momentum preserving by construction. In a recent work, Bathe [21] proposed a quite simple method of time integration for nonlinear dynamic analysis. Although energy conservation is not satisfied algorithmically by this scheme, numerical experiences carried out for the stiff pendulum example (modelled using a truss element) displayed promising results in cases in which the trapezoidal rule was unstable.

In this work a completely new nonlinear beam element is introduced. The finite element model is developed in both a classical and an energy preserving formulation. The element is able to handle large 3D rotations and displacements but small strains. The simplifications we made in the kinematics allowed to obtain quite simple compact expressions, very easy to adapt to the energy preserving scheme. This simplicity of the expressions can be considered the goal of the new formulation.

Developments are carried out in the framework of an energy preserving time integration scheme designed for multibody systems analysis, where the beam element can be used along with other mechanism finite elements like rigid bodies and several joint elements. Details of this scheme can be found in Refs. [1,2].

Examples of application for various test cases in 2D and 3D situations are presented, with comparison to results from the literature, showing the performance of the proposed new element. In particular, two examples involving the dynamic impact of a beam are shown. These examples are difficult to be solved with conventional time integration schemes because of the widely excited vibration spectrum, which includes not only axial vibration modes (as it is the case in a truss element) but also flexural vibration modes, superposed with the large displacements and rotations of the beam.

2. Classical formulation of a nonlinear beam

2.1. Kinematics of a beam

The kinematic assumptions adopted are the following:

- the beam is initially straight,
- beam cross-sections remain plane and do not deform during elastic deformation,
- shear deformation of the neutral axis is allowed,
- the rotational kinetic energy of cross-sections is taken into account.

It is also assumed that the reference configuration of the beam is chosen such that its longitudinal axis coincides with axis x_1 of the absolute frame and that its left end coincides with the frame origin. Let $(\boldsymbol{X}_0(s), \boldsymbol{R}_E)$ be the reference configuration of the beam such that

$$\boldsymbol{X}_0(s) = \frac{1}{L}(\boldsymbol{X}_B s + \boldsymbol{X}_A(L-s)) \quad s \in [0, L] \tag{1}$$

where $\boldsymbol{X}_A$, $\boldsymbol{X}_B$ are the reference positions of the beam element end nodes A and B, and $\boldsymbol{R}_E = [\,\boldsymbol{E}_1 \quad \boldsymbol{E}_2 \quad \boldsymbol{E}_3\,]$ is the rotation operator from global axes to principal axes of the cross-section of the beam (Fig. 1).

The reference configuration of a point of relative coordinates $\boldsymbol{Y} = (0, Y_2, Y_3)$ in local beam axes is

$$\boldsymbol{X}(s) = \boldsymbol{X}_0(s) + \boldsymbol{R}_E \boldsymbol{Y} \tag{2}$$

where $\boldsymbol{X}_0(s) = s\boldsymbol{E}_1$ is the reference position of a cross-section at distance s from the origin, s is the current parameter along the beam neutral axis, $\boldsymbol{R}_E\boldsymbol{Y}$ is the vector describing the material position of a point on the cross-section. The section being undeformable, Y_2 and Y_3 are constants.

After elastic deformation, and according to the hypotheses, the current configuration of the same point can be described as

$$\boldsymbol{x}(s) = \boldsymbol{X}_0(s) + \boldsymbol{u}(s) + \boldsymbol{R}(s)\boldsymbol{R}_E\boldsymbol{Y} \tag{3}$$

where $\boldsymbol{u}(s) = \boldsymbol{x}_0 - \boldsymbol{X}_0$ is the displacement of the cross-section from its reference position, being $\boldsymbol{x}_0(s)$ the new absolute position of the cross-section. This displacement field of the centerline along the beam axis is interpolated linearly as usual

$$\boldsymbol{u}(s) = N_A(s)\boldsymbol{u}_A + N_B(s)\boldsymbol{u}_B \tag{4}$$

where $N_A(s)$, $N_B(s)$ are linear shape functions, and $\boldsymbol{u}_A$, $\boldsymbol{u}_B$ are the displacements at nodes A and B of the beam. The displacements at the middle of the beam write

$$\boldsymbol{u}_{0.5} = \frac{1}{2}(\boldsymbol{u}_A + \boldsymbol{u}_B) \tag{5}$$

The rotation $\boldsymbol{R}(s)$ in Eq. (3) describes the finite rotation of the cross-section at point s from the reference to the actual configuration, i.e. the current orientation of the cross-section. Let $\boldsymbol{R}_A$ and $\boldsymbol{R}_B$ be the finite rotations (3×3 orthogonal matrices) at nodes A and B of the beam. Finite rotations are objects that lie on a curved manifold (the so called special orthogonal group SO_3) and do not form vector space. For this reason, we are not able to interpolate the rotations field as we did for the displacements (note that $\frac{1}{2}(\boldsymbol{R}_A + \boldsymbol{R}_B)$ is not orthogonal unless both rotations have a common axis).

We will express the rotation at the mid-point of the beam in the form

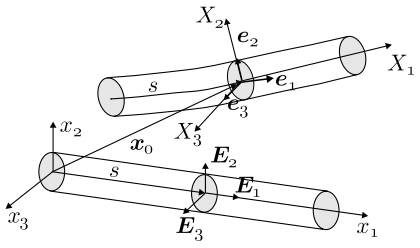

Fig. 1. Description of beam kinematics.

$$\boldsymbol{R}_{0.5} = \boldsymbol{R}_A\boldsymbol{H} = \boldsymbol{R}_B\boldsymbol{H}^{\mathrm{T}} \tag{6}$$

where the rotation increment $\boldsymbol{H}$ is written

$$\boldsymbol{H} = \sqrt{\boldsymbol{R}_A^{\mathrm{T}}\boldsymbol{R}_B} = \exp(\widetilde{\boldsymbol{\phi}}) \tag{7}$$

Here, $\boldsymbol{\phi}$ is the axial vector of three rotation parameters corresponding to the rotation $\boldsymbol{H}$ and $\widetilde{\boldsymbol{\phi}}$ the associated skew-symmetric matrix, ruled by

$$\widetilde{\boldsymbol{\phi}} = \begin{pmatrix} 0 & -\phi_3 & \phi_2 \\ \phi_3 & 0 & -\phi_1 \\ -\phi_2 & \phi_1 & 0 \end{pmatrix} \tag{8}$$

The deformation of the beam in material frame is computed as [22]

$$\boldsymbol{D}(s) = \boldsymbol{R}_E^{\mathrm{T}}\left(\boldsymbol{R}(s)^{\mathrm{T}}\frac{\mathrm{d}\boldsymbol{x}}{\mathrm{d}s} - \frac{\mathrm{d}\boldsymbol{X}}{\mathrm{d}s}\right) \tag{9}$$

which, owing to (1)–(3), can be put in the form

$$\boldsymbol{D}(s) = \boldsymbol{\Gamma}(s) + \widetilde{\boldsymbol{K}}(s)\boldsymbol{Y} \tag{10}$$

where

– $\boldsymbol{\Gamma}(s)$ is the deformation of the neutral axis

$$\boldsymbol{\Gamma}(s) = \boldsymbol{R}_E^{\mathrm{T}}\boldsymbol{R}(s)^{\mathrm{T}}\left(\boldsymbol{E}_1 + \frac{\mathrm{d}\boldsymbol{u}}{\mathrm{d}s}(s)\right) - \boldsymbol{i}_1 \tag{11}$$

with $\boldsymbol{i}_1^{\mathrm{T}} = (1 \quad 0 \quad 0)$. The deformation at the middle of the beam is thus interpolated in the form

$$\boldsymbol{\Gamma}_{0.5} = \boldsymbol{R}_E^{\mathrm{T}}\boldsymbol{R}_{0.5}^{\mathrm{T}}\left(\boldsymbol{E}_1 + \frac{\boldsymbol{u}_B - \boldsymbol{u}_A}{L}\right) - \boldsymbol{i}_1 \tag{12}$$

– $\boldsymbol{K}(s)$ is the curvature vector of the neutral axis extracted from the skew-symmetric matrix $\widetilde{\boldsymbol{K}}(s)$ and has for expression

$$\widetilde{\boldsymbol{K}}(s) = \boldsymbol{R}_E^{\mathrm{T}}\left(\boldsymbol{R}(s)^{\mathrm{T}}\frac{\mathrm{d}\boldsymbol{R}}{\mathrm{d}s}(s)\right)\boldsymbol{R}_E \tag{13}$$

By approximating the derivative of $\boldsymbol{R}$ as the difference between rotations at the beam nodes over the beam length, we may write the curvature tensor at the mid-point of the beam in the form

$$\widetilde{\boldsymbol{K}}_{0.5} = \boldsymbol{R}_E^{\mathrm{T}}\frac{\boldsymbol{H} - \boldsymbol{H}^{\mathrm{T}}}{L}\boldsymbol{R}_E \tag{14}$$

We remark that this form of computing the curvature is not fully consistent with the particular character of rotations. However, this expression may be acceptable whenever rotations at nodes A and B do not differ too much between them.

The corresponding axial curvature vector is then expressed

$$\boldsymbol{K}_{0.5} = \boldsymbol{R}_E^{\mathrm{T}}\frac{2\,\mathrm{vect}(\boldsymbol{H})}{L} \tag{15}$$

where the *vector part* of a matrix $\boldsymbol{A}$ is defined: $[\mathrm{vect}(\boldsymbol{A})]_i = \varepsilon_{ijk}A_{kj}/2$.

2.2. Rotations and derivatives of rotations at the middle of the beam

In order to compute the different terms of the beam formulation, we will need to differentiate the expressions of deformations (Eqs. (12) and (15)). Therefore, we will necessitate derivatives of the rotation operator in terms of rotation parameters at the nodes.

The middle rotation has been expressed as

$$\boldsymbol{R}_{0.5} = \boldsymbol{R}_A\boldsymbol{H} = \boldsymbol{R}_A\exp(\widetilde{\boldsymbol{\phi}}) \tag{16}$$

The variation of rotations at the middle of the beam then results

$$\delta\boldsymbol{R}_{0.5} = \boldsymbol{R}_A\delta\widetilde{\boldsymbol{\Theta}}_A\boldsymbol{H} + \boldsymbol{R}_A\boldsymbol{H}\delta\widetilde{\boldsymbol{\phi}} = \boldsymbol{R}_{0.5}\delta\widetilde{\boldsymbol{\Theta}_{0.5}} \tag{17}$$

with $\boldsymbol{\Theta}_A$, $\boldsymbol{\Theta}_{0.5}$ the axial rotation vectors corresponding to $\boldsymbol{R}_A$, $\boldsymbol{R}_{0.5}$. Therefore

$$\delta\widetilde{\boldsymbol{\Theta}}_{0.5} = \boldsymbol{R}_{0.5}^{\mathrm{T}}\boldsymbol{R}_A\delta\widetilde{\boldsymbol{\Theta}}_A\boldsymbol{H} + \delta\widetilde{\boldsymbol{\phi}} = \delta\widetilde{\boldsymbol{\phi}} + \boldsymbol{H}^{\mathrm{T}}\delta\widetilde{\boldsymbol{\Theta}}_A\boldsymbol{H} \tag{18}$$

and then, in terms of axial vectors we write

$$\delta\boldsymbol{\Theta}_{0.5} = \delta\boldsymbol{\phi} + \boldsymbol{H}^{\mathrm{T}}\delta\boldsymbol{\Theta}_A \tag{19}$$

From the definition (Eq. (7)), $\boldsymbol{H}^2 = \boldsymbol{R}_A^{\mathrm{T}}\boldsymbol{R}_B$, and therefore, the variation of $\boldsymbol{H}$ may be computed giving

$$\boldsymbol{H}\delta\boldsymbol{H} + \delta\boldsymbol{H}\boldsymbol{H} = \boldsymbol{R}_A^{\mathrm{T}}\boldsymbol{R}_B\delta\widetilde{\boldsymbol{\Theta}}_B - \delta\widetilde{\boldsymbol{\Theta}}_A\boldsymbol{R}_A^{\mathrm{T}}\boldsymbol{R}_B \tag{20}$$

Since $\delta\boldsymbol{H} = \boldsymbol{H}\delta\boldsymbol{\phi}$, then

$$\boldsymbol{H}^2\delta\widetilde{\boldsymbol{\phi}} + \boldsymbol{H}\delta\widetilde{\boldsymbol{\phi}}\boldsymbol{H} = \boldsymbol{H}^2\delta\widetilde{\boldsymbol{\Theta}}_B - \delta\widetilde{\boldsymbol{\Theta}}_A\boldsymbol{H}^2 \tag{21}$$

and in terms of axial vectors, we write

$$\delta\boldsymbol{\phi} + \boldsymbol{H}^{\mathrm{T}}\delta\boldsymbol{\phi} = \delta\boldsymbol{\Theta}_B - \boldsymbol{H}^{\mathrm{T}^2}\delta\boldsymbol{\Theta}_A \tag{22}$$

Finally, the variation of $\boldsymbol{\phi}$ may be computed as follows:

$$\delta\boldsymbol{\phi} = [\boldsymbol{I} + \boldsymbol{H}^{\mathrm{T}}]^{-1}\left(\delta\boldsymbol{\Theta}_B - \boldsymbol{H}^{\mathrm{T}^2}\delta\boldsymbol{\Theta}_A\right) \tag{23}$$

where $\boldsymbol{I}$ is the identity matrix.

By replacing the latter equation into Eq. (19), we get

$$\delta\boldsymbol{\Theta}_{0.5} = [\boldsymbol{I} + \boldsymbol{H}^{\mathrm{T}}]^{-1}\delta\boldsymbol{\Theta}_B - ([\boldsymbol{I} + \boldsymbol{H}^{\mathrm{T}}]^{-1}\boldsymbol{H}^{\mathrm{T}} - \boldsymbol{I})\boldsymbol{H}^{\mathrm{T}}\delta\boldsymbol{\Theta}_A \tag{24}$$

By noting that the following identity holds for any orthogonal matrix $\boldsymbol{H}$:

$$([\boldsymbol{I} + \boldsymbol{H}^{\mathrm{T}}]^{-1}\boldsymbol{H}^{\mathrm{T}} - \boldsymbol{I})\boldsymbol{H}^{\mathrm{T}} = [\boldsymbol{I} + \boldsymbol{H}^{\mathrm{T}}]^{-1} - \boldsymbol{I} \tag{25}$$

we finally get the expression of variations of the rotational vector at the middle of the beam

$$\delta\boldsymbol{\Theta}_{0.5} = [\boldsymbol{I} + \boldsymbol{H}^{\mathrm{T}}]^{-1}\delta\boldsymbol{\Theta}_B - ([\boldsymbol{I} + \boldsymbol{H}^{\mathrm{T}}]^{-1} - \boldsymbol{I})\delta\boldsymbol{\Theta}_A \tag{26}$$

Note that Eqs. (23) and (26) are *exact* and do not make any approximation for the evaluation of the derivatives.

Even if the beam suffers large finite rotations, we may consider that rotations at both extreme nodes are not very different between them (i.e. $\boldsymbol{R}_A \simeq \boldsymbol{R}_B$). Note that the approximation for the computation of the curvature tensor

(Eq. (14)) is based on this fact. Then, by retaining first order terms in the Taylor series expansion

$$[\boldsymbol{I}+\boldsymbol{H}^{\mathrm{T}}]^{-1}=\frac{1}{2}\boldsymbol{I}+\frac{1}{4}\left(1+\frac{1}{12}\|\boldsymbol{\phi}\|^2+\frac{1}{120}\|\boldsymbol{\phi}\|^4+\frac{17}{20\,160}\|\boldsymbol{\phi}\|^6+\cdots\right)\widetilde{\boldsymbol{\phi}} \tag{27}$$

we may write

$$\delta\boldsymbol{\Theta}_{0.5}\simeq\left[\frac{\boldsymbol{I}}{2}+\frac{\widetilde{\boldsymbol{\phi}}}{4}\right]\delta\boldsymbol{\Theta}_B+\left[\frac{\boldsymbol{I}}{2}-\frac{\widetilde{\boldsymbol{\phi}}}{4}\right]\delta\boldsymbol{\Theta}_A \tag{28}$$

By a similar reasoning, we get

$$\delta\boldsymbol{\phi}\simeq\left[\frac{\boldsymbol{I}}{2}+\frac{\widetilde{\boldsymbol{\phi}}}{4}\right]\delta\boldsymbol{\Theta}_B-\left[\frac{\boldsymbol{I}}{2}-\frac{3\widetilde{\boldsymbol{\phi}}}{4}\right]\delta\boldsymbol{\Theta}_A \tag{29}$$

2.3. Deformations variations

In order to compute the beam internal forces, we need to obtain the expressions of the derivatives of the axial strains and curvatures.

The variation of the material axial deformation $\boldsymbol{\Gamma}_{0.5}$, Eq. (12), is written

$$\delta\boldsymbol{\Gamma}_{0.5}=-\boldsymbol{R}_E^{\mathrm{T}}\delta\widetilde{\boldsymbol{\Theta}}_{0.5}\boldsymbol{R}_{0.5}^{\mathrm{T}}\left(\boldsymbol{E}_1+\frac{\boldsymbol{u}_B-\boldsymbol{u}_A}{L}\right)+\boldsymbol{R}_E^{\mathrm{T}}\boldsymbol{R}_{0.5}^{\mathrm{T}}\left(\frac{\delta\boldsymbol{u}_B-\delta\boldsymbol{u}_A}{L}\right) \tag{30}$$

If we now replace the approximation obtained for the variation of the rotation parameters at the middle of the beam, Eq. (28), we get

$$\delta\boldsymbol{\Gamma}_{0.5}=\left(\widetilde{\boldsymbol{\Gamma}_{0.5}+\boldsymbol{i}_1}\right)\boldsymbol{R}_E^{\mathrm{T}}\left[\frac{\boldsymbol{I}}{2}+\frac{\widetilde{\boldsymbol{\phi}}}{4}\right]\delta\boldsymbol{\Theta}_B+\left(\widetilde{\boldsymbol{\Gamma}_{0.5}+\boldsymbol{i}_1}\right)\boldsymbol{R}_E^{\mathrm{T}}\left[\frac{\boldsymbol{I}}{2}-\frac{\widetilde{\boldsymbol{\phi}}}{4}\right]\delta\boldsymbol{\Theta}_A+\boldsymbol{R}_E^{\mathrm{T}}\boldsymbol{R}^{\mathrm{T}}\left(\frac{\delta\boldsymbol{u}_B-\delta\boldsymbol{u}_A}{L}\right) \tag{31}$$

By differentiating Eq. (15), the variation of the curvatures axial vector at the beam mid-point may be written as follows:

$$\delta\boldsymbol{K}_{0.5}=\boldsymbol{R}_E^{\mathrm{T}}\left[\frac{\boldsymbol{H}^{\mathrm{T}}-\mathrm{tr}(\boldsymbol{H})\boldsymbol{I}}{L}\right]\delta\boldsymbol{\phi}=\frac{\boldsymbol{R}_E^{\mathrm{T}}}{L}\overline{\mathrm{dev}}[\boldsymbol{H}^{\mathrm{T}}]\delta\boldsymbol{\phi} \tag{32}$$

where $\overline{\mathrm{dev}}[\boldsymbol{H}]=\boldsymbol{H}-\mathrm{tr}(\boldsymbol{H})\boldsymbol{I}$. By using Taylor series developments, we may express $\boldsymbol{H}^{\mathrm{T}}$ and $\mathrm{tr}(\boldsymbol{H})$ in the form

$$\begin{aligned}\boldsymbol{H}^{\mathrm{T}}&=\boldsymbol{I}-\widetilde{\boldsymbol{\phi}}+\frac{1}{2!}\widetilde{\boldsymbol{\phi}}^2-\frac{1}{3!}\widetilde{\boldsymbol{\phi}}^3+\cdots\\ \mathrm{tr}(\boldsymbol{H})&=3-\|\boldsymbol{\phi}\|^2+\frac{1}{6}\|\boldsymbol{\phi}\|^4+\cdots\end{aligned} \tag{33}$$

Then, after replacement into Eq. (32), and by using Eq. (29), we get

$$\begin{aligned}\delta\boldsymbol{K}_{0.5}&=-\frac{2\boldsymbol{R}_E^{\mathrm{T}}}{L}\left[\boldsymbol{I}+\frac{\widetilde{\boldsymbol{\phi}}}{2}+\cdots\right]\delta\boldsymbol{\phi}\\&=\frac{\boldsymbol{R}_E^{\mathrm{T}}}{L}\left\{-\left[\boldsymbol{I}-\widetilde{\boldsymbol{\phi}}\right]\delta\boldsymbol{\Theta}_A+[\boldsymbol{I}+\widetilde{\boldsymbol{\phi}}]\delta\boldsymbol{\Theta}_B\right\}\end{aligned} \tag{34}$$

From now on, we will omit the index 0.5 and notate directly $\boldsymbol{\Gamma}$, $\boldsymbol{K}$, ... for quantities evaluated at the middle of the beam.

Note that $\boldsymbol{K}=2\boldsymbol{R}_E^{\mathrm{T}}\boldsymbol{\phi}/L$, and therefore

$$\boldsymbol{R}_E^{\mathrm{T}}\boldsymbol{\phi}=\frac{L}{2}\boldsymbol{K} \tag{35}$$

By replacing the latter equation into Eqs. (31) and (34), we obtain the final expression of the variation of axial deformation $\boldsymbol{\Gamma}$ and curvature $\boldsymbol{K}$ at the mid-point

$$\begin{aligned}\delta\boldsymbol{\Gamma}&=\left(\frac{\widetilde{\boldsymbol{\Gamma}+\boldsymbol{i}_1}}{2}\right)\left[\boldsymbol{I}+\frac{L\widetilde{\boldsymbol{K}}}{4}\right]\boldsymbol{R}_E^{\mathrm{T}}\delta\boldsymbol{\Theta}_B+\left(\frac{\widetilde{\boldsymbol{\Gamma}+\boldsymbol{i}_1}}{2}\right)\left[\boldsymbol{I}-\frac{L\widetilde{\boldsymbol{K}}}{4}\right]\boldsymbol{R}_E^{\mathrm{T}}\delta\boldsymbol{\Theta}_A\\&\quad+\boldsymbol{R}_E^{\mathrm{T}}\boldsymbol{R}^{\mathrm{T}}\left(\frac{\delta\boldsymbol{u}_B-\delta\boldsymbol{u}_A}{L}\right)\\ \delta\boldsymbol{K}&=-\left[\frac{\boldsymbol{I}}{L}-\frac{\widetilde{\boldsymbol{K}}}{2}\right]\boldsymbol{R}_E^{\mathrm{T}}\delta\boldsymbol{\Theta}_A+\left[\frac{\boldsymbol{I}}{L}+\frac{\widetilde{\boldsymbol{K}}}{2}\right]\boldsymbol{R}_E^{\mathrm{T}}\delta\boldsymbol{\Theta}_B\end{aligned} \tag{36}$$

If we now define matrix $\boldsymbol{B}$ which relates strains variations at the mid-point with variations of nodal displacements and rotations

$$\boldsymbol{B}^{\mathrm{T}}=\begin{pmatrix}-\frac{\boldsymbol{R}\boldsymbol{R}_E}{L} & 0\\ -\frac{1}{2}\boldsymbol{R}_E\left[\boldsymbol{I}+\frac{L}{4}\widetilde{\boldsymbol{K}}\right]\left(\widetilde{\boldsymbol{\Gamma}+\boldsymbol{i}_1}\right) & -\frac{\boldsymbol{R}_E}{L}\left[\boldsymbol{I}+\frac{L}{2}\widetilde{\boldsymbol{K}}\right]\\ \frac{\boldsymbol{R}\boldsymbol{R}_E}{L} & 0\\ -\frac{1}{2}\boldsymbol{R}_E\left[\boldsymbol{I}-\frac{L}{4}\widetilde{\boldsymbol{K}}\right](\widetilde{\boldsymbol{\Gamma}+\boldsymbol{i}_1}) & \frac{\boldsymbol{R}_E}{L}\left[\boldsymbol{I}-\frac{L}{2}\widetilde{\boldsymbol{K}}\right]\end{pmatrix} \tag{37}$$

we may write the deformation variations in the form

$$\begin{pmatrix}\delta\boldsymbol{\Gamma}\\ \delta\boldsymbol{K}\end{pmatrix}=\boldsymbol{B}\delta\boldsymbol{q}=\boldsymbol{B}\begin{pmatrix}\delta\boldsymbol{u}_A\\ \delta\boldsymbol{\Theta}_A\\ \delta\boldsymbol{u}_B\\ \delta\boldsymbol{\Theta}_B\end{pmatrix} \tag{38}$$

2.4. Discretized form of the dynamic equilibrium equations

The discretized form of the internal virtual work takes the form

$$\begin{aligned}\delta\mathscr{W}_{\mathrm{int}}&=\int_0^L(\boldsymbol{N}^{\mathrm{T}}\delta\boldsymbol{\Gamma}+\boldsymbol{M}^{\mathrm{T}}\delta\boldsymbol{K})\mathrm{d}s=\int_0^L\delta\boldsymbol{q}^{\mathrm{T}}\boldsymbol{B}^{\mathrm{T}}\boldsymbol{\Sigma}\,\mathrm{d}s\\&=\delta\boldsymbol{q}^{\mathrm{T}}\boldsymbol{F}_{\mathrm{int}}\end{aligned} \tag{39}$$

with the internal forces

$$\boldsymbol{F}_{\mathrm{int}}=\int_0^L\boldsymbol{B}^{\mathrm{T}}\boldsymbol{\Sigma}\,\mathrm{d}s \tag{40}$$

The virtual work of external forces may be put in a similar discretized form

$$\delta\mathscr{W}_{\mathrm{ext}}=\delta\boldsymbol{q}^{\mathrm{T}}\boldsymbol{F}_{\mathrm{ext}} \tag{41}$$

Finally, the virtual work of the inertia forces

$$\delta\mathscr{W}_{\text{iner}} = \int_0^L \left(\mu\ddot{\boldsymbol{x}}_0^{\mathrm{T}}\delta\boldsymbol{x}_0 + (\boldsymbol{J}\dot{\boldsymbol{\Omega}} + \widetilde{\boldsymbol{\Omega}}\boldsymbol{J}\boldsymbol{\Omega})^{\mathrm{T}}\delta\boldsymbol{\Theta}\right)\mathrm{d}s \tag{42}$$

is also discretized in terms of displacement parameters. We have

$$\delta\mathscr{W}_{\text{iner}} = \delta\boldsymbol{q}^{\mathrm{T}}\boldsymbol{F}_{\text{iner}} \tag{43}$$

where the discretized inertia loads take the following form:

$$\boldsymbol{F}_{\text{iner}} = \int_0^L \boldsymbol{P}(s)^{\mathrm{T}}\begin{bmatrix}\mu\ddot{\boldsymbol{x}}_0 \\ \boldsymbol{T}^{\mathrm{T}}(\boldsymbol{J}\dot{\boldsymbol{\Omega}} + \widetilde{\boldsymbol{\Omega}}\boldsymbol{J}\boldsymbol{\Omega})\end{bmatrix}\mathrm{d}s \tag{44}$$

in which $\boldsymbol{P}(s)$ is the matrix of shape functions

$$\boldsymbol{P}(s) = \begin{bmatrix} N_1\boldsymbol{I} & 0 & N_2\boldsymbol{I} & 0 \\ 0 & N_1\boldsymbol{I} & 0 & N_2\boldsymbol{I}\end{bmatrix} \tag{45}$$

Velocities are treated as *quasi-coordinates*, i.e. they take the form of linear combinations of generalized coordinate time derivatives

$$\boldsymbol{v} = \boldsymbol{T}(\boldsymbol{q})\dot{\boldsymbol{q}} = \begin{bmatrix}\dot{\boldsymbol{x}} \\ \boldsymbol{\Omega}\end{bmatrix} \tag{46}$$

$\boldsymbol{T}$ is the tangent operator, function of the adopted rotation parameters. By adopting Euler parameters, the $\boldsymbol{T}$ operator is defined by the following expression:

$$\boldsymbol{T}(\boldsymbol{e}) = 2\left(e_0\boldsymbol{I} + \frac{1}{e_0}\boldsymbol{e}\boldsymbol{e}^{\mathrm{T}} - \widetilde{\boldsymbol{e}}\right) \tag{47}$$

Let us now split the expression (44) of inertia forces into relative and gyroscopic inertia forces

$$\boldsymbol{F}_{\text{iner}} = \boldsymbol{F}_{\text{rel}} + \boldsymbol{F}_{\text{gyro}} \tag{48}$$

The relative inertia forces are those involving the second time derivatives of the parameters and may be expressed in terms of a mass matrix

$$\boldsymbol{F}_{\text{rel}} = \boldsymbol{M}\ddot{\boldsymbol{q}} \tag{49}$$

with the expression of the tangent mass matrix

$$\boldsymbol{M} = \int_0^L \boldsymbol{P}(s)^{\mathrm{T}}\begin{bmatrix} m\boldsymbol{I} & 0 \\ 0 & \boldsymbol{T}^{\mathrm{T}}\boldsymbol{J}\boldsymbol{T}\end{bmatrix}\boldsymbol{P}(s)\mathrm{d}s \tag{50}$$

where $\boldsymbol{J}$ is the material expression of the inertia of the cross-section.

The gyroscopic inertia forces collect the missing terms

$$\boldsymbol{F}_{\text{gyro}} = \int_0^L \boldsymbol{P}(s)^{\mathrm{T}}\begin{bmatrix}0 \\ \boldsymbol{T}^{\mathrm{T}}(\boldsymbol{J}\dot{\boldsymbol{T}} + \widetilde{\boldsymbol{\Omega}}\boldsymbol{J}\boldsymbol{T})\dot{\boldsymbol{e}}\end{bmatrix}\mathrm{d}s \tag{51}$$

The last results allow us to express the dynamic equilibrium virtual work expression in the condensed form

$$\delta\boldsymbol{q}^{\mathrm{T}}[\boldsymbol{F}_{\text{int}} + \boldsymbol{F}_{\text{iner}} - \boldsymbol{F}_{\text{ext}}] = 0 \tag{52}$$

For arbitrary kinematically admissible displacement variations, and provided that the end loads include the reaction forces from neighbouring elements, equilibrium of the beam element is obtained in the form

$$\boldsymbol{F}_{\text{int}} + \boldsymbol{F}_{\text{rel}} + \boldsymbol{F}_{\text{gyro}} - \boldsymbol{F}_{\text{ext}} = 0 \tag{53}$$

2.5. Deformation energy

The strain energy is computed by integrating the density of strain energy along the beam length. This integral may be approximated using one Gauss point at the middle of the beam, giving

$$\mathscr{V} = \frac{1}{2}\int_0^L \begin{pmatrix}\boldsymbol{\Gamma}(s) \\ \boldsymbol{K}(s)\end{pmatrix}\cdot\boldsymbol{C}\begin{pmatrix}\boldsymbol{\Gamma}(s) \\ \boldsymbol{K}(s)\end{pmatrix}\mathrm{d}s \simeq \frac{1}{2}\begin{pmatrix}\boldsymbol{\Gamma} \\ \boldsymbol{K}\end{pmatrix}\cdot\boldsymbol{C}\begin{pmatrix}\boldsymbol{\Gamma} \\ \boldsymbol{K}\end{pmatrix}L \tag{54}$$

where $\boldsymbol{C}$ is the matrix of elastic coefficients, which may takes usually the form

$$\boldsymbol{C} = \mathrm{diag}(\,EA \quad GA_2 \quad GA_3 \quad GJ \quad EI_2 \quad EI_3\,) \tag{55}$$

Here EA is the axial stiffness, GA_2 and GA_3 are the shear bending stiffnesses along the transverse axes, GJ is the torsional stiffness and EI_2 and EI_3 are the bending stiffnesses.

The internal forces are evaluated by differentiation of the strain energy of the element

$$\delta\mathscr{V} = \begin{pmatrix}\delta\boldsymbol{\Gamma} \\ \delta\boldsymbol{K}\end{pmatrix}\cdot\boldsymbol{C}\boldsymbol{L}\begin{pmatrix}\boldsymbol{\Gamma} \\ \boldsymbol{K}\end{pmatrix} = \begin{pmatrix}\delta\boldsymbol{u}_A \\ \delta\boldsymbol{\Theta}_A \\ \delta\boldsymbol{u}_B \\ \delta\boldsymbol{\Theta}_B\end{pmatrix}\cdot\boldsymbol{F}_{\text{int}} \tag{56}$$

After replacing Eq. (38) in the latter, we get the expression of the vector of internal forces of the beam

$$\boldsymbol{F}_{\text{int}} = \boldsymbol{B}^{\mathrm{T}}\begin{pmatrix}\boldsymbol{N} \\ \boldsymbol{M}\end{pmatrix}L = \begin{pmatrix} -\boldsymbol{R}\boldsymbol{R}_E\boldsymbol{N} \\ -\frac{1}{2}\boldsymbol{R}_E\left[\boldsymbol{I} + \frac{L}{4}\widetilde{\boldsymbol{K}}\right](\boldsymbol{\Gamma}\widetilde{+\boldsymbol{i}}_1)\boldsymbol{N}L - \boldsymbol{R}_E\left[\boldsymbol{I} + \frac{L}{2}\widetilde{\boldsymbol{K}}\right]\boldsymbol{M} \\ \boldsymbol{R}\boldsymbol{R}_E\boldsymbol{N} \\ -\frac{1}{2}\boldsymbol{R}_E\left[\boldsymbol{I} - \frac{L}{4}\widetilde{\boldsymbol{K}}\right](\boldsymbol{\Gamma}\widetilde{+\boldsymbol{i}}_1)\boldsymbol{N}L + \boldsymbol{R}_E\left[\boldsymbol{I} - \frac{L}{2}\widetilde{\boldsymbol{K}}\right]\boldsymbol{M}\end{pmatrix} \tag{57}$$

where $\begin{pmatrix}\boldsymbol{N} \\ \boldsymbol{M}\end{pmatrix} = \boldsymbol{C}\begin{pmatrix}\boldsymbol{\Gamma} \\ \boldsymbol{K}\end{pmatrix}$ is the vector of internal efforts and moments at the middle point evaluated in material axes.

After differentiating the internal forces vector, we get the tangent stiffness $\boldsymbol{S}$

$$D\boldsymbol{F}_{\text{int}}\cdot\Delta\boldsymbol{q} = \boldsymbol{S}\Delta\boldsymbol{q} = \boldsymbol{B}^{\mathrm{T}}\boldsymbol{C}\boldsymbol{L}\boldsymbol{B}\begin{pmatrix}\Delta\boldsymbol{u}_A \\ \Delta\boldsymbol{\Theta}_A \\ \Delta\boldsymbol{u}_B \\ \Delta\boldsymbol{\Theta}_B\end{pmatrix} + (D\boldsymbol{B}^{\mathrm{T}}\Delta\boldsymbol{q})\cdot L\begin{pmatrix}\boldsymbol{N} \\ \boldsymbol{M}\end{pmatrix} \tag{58}$$

The first term on the RHS is the so-called material tangent matrix

$$\boldsymbol{S}_{\text{mat}} = \boldsymbol{B}^{\mathrm{T}}\boldsymbol{C}\boldsymbol{L}\boldsymbol{B} \tag{59}$$

The second term on the RHS of Eq. (58) is the geometric stiffness matrix, which may be written in the form

$$\boldsymbol{S}_{\text{geo}}\Delta\boldsymbol{q} = D|_{N,M}\left(\boldsymbol{B}^{\mathrm{T}}L\begin{pmatrix}\boldsymbol{N}\\ \boldsymbol{M}\end{pmatrix}\right)\cdot\Delta\boldsymbol{q} \tag{60}$$

where $D|_{N,M}\{\}\cdot\Delta\boldsymbol{q}$ denotes the Frechet derivative along the direction $\Delta\boldsymbol{q}$ with $\boldsymbol{N}$, $\boldsymbol{M}$ held constant.

The following derivatives may be verified by performing some algebra:

$$\begin{aligned}
&D|_{N,M}(-\boldsymbol{R}\boldsymbol{R}_E\boldsymbol{N})\cdot\Delta\boldsymbol{q}\\
&\quad=\frac{1}{2}\boldsymbol{R}\boldsymbol{R}_E\widetilde{\boldsymbol{N}}\left[\boldsymbol{I}-\frac{L\widetilde{\boldsymbol{K}}}{4}\right]\boldsymbol{R}_E^{\mathrm{T}}\Delta\boldsymbol{\Theta}_A-\frac{1}{2}\boldsymbol{R}\boldsymbol{R}_E\widetilde{\boldsymbol{N}}\left[\boldsymbol{I}+\frac{L\widetilde{\boldsymbol{K}}}{4}\right]\boldsymbol{R}_E^{\mathrm{T}}\Delta\boldsymbol{\Theta}_B
\end{aligned}\tag{61}$$

$$\begin{aligned}
&D|_{N,M}\left(-\frac{1}{2}\boldsymbol{R}_E\left[\boldsymbol{I}+\frac{L}{4}\widetilde{\boldsymbol{K}}\right]\widetilde{(\boldsymbol{\Gamma}+\boldsymbol{i}_1)}\boldsymbol{N}L\right)\cdot\Delta\boldsymbol{q}\\
&\quad=\frac{1}{2}\boldsymbol{R}_E\left[\boldsymbol{I}+\frac{L}{4}\widetilde{\boldsymbol{K}}\right]\widetilde{\boldsymbol{N}}\boldsymbol{R}_E^{\mathrm{T}}\boldsymbol{R}^{\mathrm{T}}\Delta\boldsymbol{u}_A\\
&\qquad+\boldsymbol{R}_E\left(\left[\boldsymbol{I}+\frac{L}{4}\widetilde{\boldsymbol{K}}\right]\widetilde{\boldsymbol{N}}\widetilde{(\boldsymbol{\Gamma}+\boldsymbol{i}_1)}\left[\boldsymbol{I}-\frac{L}{4}\widetilde{\boldsymbol{K}}\right]\right.\\
&\qquad\left.-\frac{1}{2}\left[\widetilde{(\boldsymbol{\Gamma}+\boldsymbol{i}_1)}\times\boldsymbol{N}\right]\left[\boldsymbol{I}-\frac{L}{2}\widetilde{\boldsymbol{K}}\right]\right)\boldsymbol{R}_E^{\mathrm{T}}\frac{L}{4}\Delta\boldsymbol{\Theta}_A\\
&\qquad-\frac{1}{2}\boldsymbol{R}_E\left[\boldsymbol{I}+\frac{L}{4}\widetilde{\boldsymbol{K}}\right]\widetilde{\boldsymbol{N}}\boldsymbol{R}_E^{\mathrm{T}}\boldsymbol{R}^{\mathrm{T}}\Delta\boldsymbol{u}_B\\
&\qquad-\boldsymbol{R}_E\left(\left[\boldsymbol{I}+\frac{L}{4}\widetilde{\boldsymbol{K}}\right]\widetilde{\boldsymbol{N}}\widetilde{(\boldsymbol{\Gamma}+\boldsymbol{i}_1)}\left[\boldsymbol{I}+\frac{L}{4}\widetilde{\boldsymbol{K}}\right]\right.\\
&\qquad\left.+\frac{1}{2}\left[\widetilde{(\boldsymbol{\Gamma}+\boldsymbol{i}_1)}\times\boldsymbol{N}\right]\left[\boldsymbol{I}+\frac{L}{2}\widetilde{\boldsymbol{K}}\right]\right)\boldsymbol{R}_E^{\mathrm{T}}\frac{L}{4}\Delta\boldsymbol{\Theta}_B
\end{aligned}\tag{62}$$

$$\begin{aligned}
&D|_{N,M}\left(-\boldsymbol{R}_E\left[\boldsymbol{I}+\frac{L}{2}\widetilde{\boldsymbol{K}}\right]\boldsymbol{M}\right)\cdot\Delta\boldsymbol{q}\\
&\quad=\frac{1}{2}\boldsymbol{R}_E\widetilde{\boldsymbol{M}}\left[\boldsymbol{I}-\frac{L}{2}\widetilde{\boldsymbol{K}}\right]\boldsymbol{R}_E^{\mathrm{T}}\Delta\boldsymbol{\Theta}_A+\frac{1}{2}\boldsymbol{R}_E\widetilde{\boldsymbol{M}}\left[\boldsymbol{I}+\frac{L}{2}\widetilde{\boldsymbol{K}}\right]\boldsymbol{R}_E^{\mathrm{T}}\Delta\boldsymbol{\Theta}_B
\end{aligned}\tag{63}$$

Then, the geometric stiffness matrix is expressed as follows:

$$\boldsymbol{S}_{\text{geo}}=\begin{pmatrix}\boldsymbol{S}_{gu_Au_A} & \boldsymbol{S}_{gu_A\Theta_A} & \boldsymbol{S}_{gu_Au_B} & \boldsymbol{S}_{gu_A\Theta_B}\\ & \boldsymbol{S}_{g\Theta_A\Theta_A} & \boldsymbol{S}_{g\Theta_Au_B} & \boldsymbol{S}_{g\Theta_A\Theta_B}\\ & & \boldsymbol{S}_{gu_Bu_B} & \boldsymbol{S}_{gu_B\Theta_B}\\ \text{symm} & & & \boldsymbol{S}_{g\Theta_B\Theta_B}\end{pmatrix}\tag{64}$$

where

$$\boldsymbol{S}_{gu_Au_A}=0$$

$$\boldsymbol{S}_{gu_A\Theta_A}=\frac{1}{2}\boldsymbol{R}\boldsymbol{R}_E\widetilde{\boldsymbol{N}}\left[\boldsymbol{I}-\frac{L}{4}\widetilde{\boldsymbol{K}}\right]\boldsymbol{R}_E^{\mathrm{T}}$$

$$\boldsymbol{S}_{gu_Au_B}=0$$

$$\boldsymbol{S}_{gu_A\Theta_B}=-\frac{1}{2}\boldsymbol{R}\boldsymbol{R}_E\widetilde{\boldsymbol{N}}\left[\boldsymbol{I}+\frac{L}{4}\widetilde{\boldsymbol{K}}\right]\boldsymbol{R}_E^{\mathrm{T}}$$

$$\begin{aligned}
\boldsymbol{S}_{g\Theta_A\Theta_A}=\boldsymbol{R}_E\left(\left[\boldsymbol{I}+\frac{L}{4}\widetilde{\boldsymbol{K}}\right]\widetilde{\boldsymbol{N}}\widetilde{(\boldsymbol{\Gamma}+\boldsymbol{i}_1)}\left[\boldsymbol{I}-\frac{L}{4}\widetilde{\boldsymbol{K}}\right]\right.\\
\left.-\frac{1}{2}\left[\widetilde{(\boldsymbol{\Gamma}+\boldsymbol{i}_1)}\times\boldsymbol{N}+\frac{4}{L}\widetilde{\boldsymbol{M}}\right]\left[\boldsymbol{I}-\frac{L}{2}\widetilde{\boldsymbol{K}}\right]\right)\boldsymbol{R}_E^{\mathrm{T}}\frac{L}{4}
\end{aligned}$$

$$\boldsymbol{S}_{g\Theta_Au_B}=\frac{1}{2}\boldsymbol{R}_E\left[\boldsymbol{I}+\frac{L}{4}\widetilde{\boldsymbol{K}}\right]\widetilde{\boldsymbol{N}}\boldsymbol{R}_E^{\mathrm{T}}\boldsymbol{R}^{\mathrm{T}}=-\boldsymbol{S}_{gu_A\Theta_A}^{\mathrm{T}}$$

$$\begin{aligned}
\boldsymbol{S}_{g\Theta_A\Theta_B}=\boldsymbol{R}_E\left(\left[\boldsymbol{I}+\frac{L}{4}\widetilde{\boldsymbol{K}}\right]\widetilde{\boldsymbol{N}}\widetilde{(\boldsymbol{\Gamma}+\boldsymbol{i}_1)}\left[\boldsymbol{I}+\frac{L}{4}\widetilde{\boldsymbol{K}}\right]\right.\\
\left.+\frac{1}{2}\left[\widetilde{(\boldsymbol{\Gamma}+\boldsymbol{i}_1)}\times\boldsymbol{N}+\frac{4}{L}\widetilde{\boldsymbol{M}}\right]\left[\boldsymbol{I}+\frac{L}{2}\widetilde{\boldsymbol{K}}\right]\right)\boldsymbol{R}_E^{\mathrm{T}}\frac{L}{4}
\end{aligned}$$

$$\boldsymbol{S}_{gu_Bu_B}=0$$

$$\boldsymbol{S}_{gu_B\Theta_B}=\frac{1}{2}\boldsymbol{R}\boldsymbol{R}_E\widetilde{\boldsymbol{N}}\left[\boldsymbol{I}+\frac{L}{4}\widetilde{\boldsymbol{K}}\right]\boldsymbol{R}_E^{\mathrm{T}}=-\boldsymbol{S}_{gu_A\Theta_B}$$

$$\begin{aligned}
\boldsymbol{S}_{g\Theta_B\Theta_B}=\boldsymbol{R}_E\left(\left[\boldsymbol{I}-\frac{L}{4}\widetilde{\boldsymbol{K}}\right]\widetilde{\boldsymbol{N}}\widetilde{(\boldsymbol{\Gamma}+\boldsymbol{i}_1)}\left[\boldsymbol{I}+\frac{L}{4}\widetilde{\boldsymbol{K}}\right]\right.\\
\left.-\frac{1}{2}\left[\widetilde{(\boldsymbol{\Gamma}+\boldsymbol{i}_1)}\times\boldsymbol{N}-\frac{4}{L}\widetilde{\boldsymbol{M}}\right]\left[\boldsymbol{I}+\frac{L}{2}\widetilde{\boldsymbol{K}}\right]\right)\boldsymbol{R}_E^{\mathrm{T}}\frac{L}{4}
\end{aligned}$$

3. Formulation of a beam with energy conservation

The energy preserving time integration scheme that serves as framework for the development of our energy preserving beam element was presented elsewhere [22,1,2]. The scheme is based on the application of the mid-point rule to the rate equations for the generalized coordinates $\boldsymbol{q}$ and velocities $\boldsymbol{v}$ leading to the following relationships:

$$\dot{\boldsymbol{q}}_{n+\frac{1}{2}}=\frac{1}{h}(\boldsymbol{q}_{n+1}-\boldsymbol{q}_n),\quad \dot{\boldsymbol{v}}_{n+\frac{1}{2}}=\frac{1}{h}(\boldsymbol{v}_{n+1}-\boldsymbol{v}_n)\tag{65}$$

By making use of these equations we discretize in time the equilibrium equation (53) in the form

$$\boldsymbol{F}_{\text{int}_{n+\frac{1}{2}}}+\boldsymbol{F}_{\text{rel}_{n+\frac{1}{2}}}+\boldsymbol{F}_{\text{gyro}_{n+\frac{1}{2}}}-\boldsymbol{F}_{\text{ext}_{n+\frac{1}{2}}}=0\tag{66}$$

Next we will find the corresponding expressions for each term of the equilibrium equation, to finally demonstrate the energy preservation of the proposed formulation in the absence of non-conservative external forces.

3.1. Computation of the time discrete inertia terms

The inertia terms are computed by following a corotational approach, obtaining expressions for the mass matrix and the gyroscopic and inertia forces that have a similar pattern as that of a rigid body model (see [22,1,2]).

By adopting linear shape functions N_1 and N_2 in the $\boldsymbol{P}(s)$ matrix of Eq. (45), the corresponding mid-point expressions result

$$\begin{aligned}
\boldsymbol{M}_{n+\frac{1}{2}}&=\boldsymbol{T}_{n+\frac{1}{2}}\int_0^L\boldsymbol{P}(s)^{\mathrm{T}}\begin{bmatrix}m\boldsymbol{I} & 0\\ 0 & \boldsymbol{J}\end{bmatrix}\boldsymbol{P}(s)\mathrm{d}s\\
&=\frac{L}{6}\begin{bmatrix}2m\boldsymbol{I} & 0 & m\boldsymbol{I} & 0\\ 0 & 4\boldsymbol{J} & 0 & 2\boldsymbol{J}\\ m\boldsymbol{I} & 0 & 2m\boldsymbol{I} & 0\\ 0 & 2\boldsymbol{J} & 0 & 4\boldsymbol{J}\end{bmatrix}
\end{aligned}\tag{67}$$

$$\boldsymbol{F}_{\mathrm{rel}_{n+\frac{1}{2}}} = \boldsymbol{M}_{n+\frac{1}{2}}\boldsymbol{a}_{n+\frac{1}{2}} = \frac{L}{6}\begin{bmatrix} m\left(2\boldsymbol{a}_{A_{n+\frac{1}{2}}} + \boldsymbol{a}_{B_{n+\frac{1}{2}}}\right) \\ 2\boldsymbol{J}\left(2\boldsymbol{A}_{A_{n+\frac{1}{2}}} + \boldsymbol{A}_{B_{n+\frac{1}{2}}}\right) \\ m\left(\boldsymbol{a}_{A_{n+\frac{1}{2}}} + 2\boldsymbol{a}_{B_{n+\frac{1}{2}}}\right) \\ 2\boldsymbol{J}\left(\boldsymbol{A}_{A_{n+\frac{1}{2}}} + 2\boldsymbol{A}_{B_{n+\frac{1}{2}}}\right) \end{bmatrix} \tag{68}$$

being $\boldsymbol{a}_{i_{n+\frac{1}{2}}}$ and $\boldsymbol{A}_{i_{n+\frac{1}{2}}}$ the translational and rotational acceleration vectors of the i node at time $t = n+\frac{1}{2}$

$$\boldsymbol{F}_{\mathrm{gyro}_{n+\frac{1}{2}}} = \begin{bmatrix} \boldsymbol{T}^{\mathrm{T}}_{n+\frac{1}{2}} & 0 \\ 0 & \boldsymbol{T}^{\mathrm{T}}_{n+\frac{1}{2}} \end{bmatrix}\frac{L}{6}\begin{bmatrix} 0 \\ \widetilde{\boldsymbol{\Omega}}_{A_{n+\frac{1}{2}}}\boldsymbol{J}\left(2\boldsymbol{\Omega}_{A_{n+\frac{1}{2}}} + \boldsymbol{\Omega}_{B_{n+\frac{1}{2}}}\right) \\ 0 \\ \widetilde{\boldsymbol{\Omega}}_{B_{n+\frac{1}{2}}}\boldsymbol{J}\left(\boldsymbol{\Omega}_{A_{n+\frac{1}{2}}} + 2\boldsymbol{\Omega}_{B_{n+\frac{1}{2}}}\right) \end{bmatrix} \tag{69}$$

The mid-point gyroscopic forces can also be expressed as

$$\boldsymbol{F}_{\mathrm{gyro}_{n+\frac{1}{2}}} = \frac{1}{h}\boldsymbol{G}_{n+\frac{1}{2}}(\boldsymbol{q}_{n+1} - \boldsymbol{q}_n) \tag{70}$$

where the mid-point expression of the skew-symmetric matrix $\boldsymbol{G}$ for the beam element writes

$$\boldsymbol{G}_{n+\frac{1}{2}} = \begin{bmatrix} 0 & 0 & 0 & 0 \\ 0 & -\frac{2L}{3}\left(\boldsymbol{J}\left(2\widetilde{\boldsymbol{\Omega}_{A_{n+\frac{1}{2}}} + \boldsymbol{\Omega}_{B_{n+\frac{1}{2}}}}\right)\right) & 0 & 0 \\ 0 & 0 & 0 & 0 \\ 0 & 0 & 0 & \frac{2L}{3}\left(\boldsymbol{J}\left(\widetilde{\boldsymbol{\Omega}_{A_{n+\frac{1}{2}}} + 2\boldsymbol{\Omega}_{B_{n+\frac{1}{2}}}}\right)\right) \end{bmatrix} \tag{71}$$

3.2. Computation of the time discrete internal forces

The key aspect in achieving energy conservation for the beam is the computation of internal stresses at the mid-point in time. Indeed, when the mid-point rule is applied for time integration the work produced by the discrete internal forces of Eq. (52) takes the form $\boldsymbol{F}^{\mathrm{T}*}_{\mathrm{int}_{n+\frac{1}{2}}}(\boldsymbol{q}_{n+1} - \boldsymbol{q}_n)$. The vector of discrete internal forces at $t_{n+\frac{1}{2}}$ is constructed in order to satisfy the following condition:

$$(\boldsymbol{q}_{n+1} - \boldsymbol{q}_n)^{\mathrm{T}}\boldsymbol{F}^{*}_{\mathrm{int}_{n+\frac{1}{2}}} = \mathscr{V}_{n+1} - \mathscr{V}_n \tag{72}$$

The strain energy of the beam has the expression

$$\mathscr{V} = \frac{1}{2}\begin{pmatrix}\boldsymbol{N}\\ \boldsymbol{M}\end{pmatrix}\cdot\begin{pmatrix}\boldsymbol{\Gamma}\\ \boldsymbol{K}\end{pmatrix}L \tag{73}$$

and therefore

$$\begin{aligned}\mathscr{V}_{n+1} - \mathscr{V}_n &= \frac{L}{2}\left[\begin{pmatrix}\boldsymbol{N}\\ \boldsymbol{M}\end{pmatrix}_{n+1}\cdot\begin{pmatrix}\boldsymbol{\Gamma}\\ \boldsymbol{K}\end{pmatrix}_{n+1} - \begin{pmatrix}\boldsymbol{N}\\ \boldsymbol{M}\end{pmatrix}_{n}\cdot\begin{pmatrix}\boldsymbol{\Gamma}\\ \boldsymbol{K}\end{pmatrix}_{n}\right] \\ &= \begin{pmatrix}\boldsymbol{N}\\ \boldsymbol{M}\end{pmatrix}_{n+\frac{1}{2}}\cdot\left[\begin{pmatrix}\boldsymbol{\Gamma}\\ \boldsymbol{K}\end{pmatrix}_{n+1} - \begin{pmatrix}\boldsymbol{\Gamma}\\ \boldsymbol{K}\end{pmatrix}_{n}\right]L\end{aligned} \tag{74}$$

Then, if we build a strain matrix $\boldsymbol{B}_{n+\frac{1}{2}}$ (using the *discrete directional derivative* concept of Gonzalez [23,24]) such that

$$\begin{pmatrix}\boldsymbol{\Gamma}\\ \boldsymbol{K}\end{pmatrix}_{n+1} - \begin{pmatrix}\boldsymbol{\Gamma}\\ \boldsymbol{K}\end{pmatrix}_{n} = \boldsymbol{B}_{n+\frac{1}{2}}(\boldsymbol{q}_{n+1} - \boldsymbol{q}_n) \tag{75}$$

energy will be preserved provided internal forces at the mid-point are computed in the averaged form

$$\boldsymbol{F}^{*}_{\mathrm{int}_{n+\frac{1}{2}}} = \boldsymbol{B}^{\mathrm{T}}_{n+\frac{1}{2}}\begin{pmatrix}\boldsymbol{N}\\ \boldsymbol{M}\end{pmatrix}_{n+\frac{1}{2}}L \tag{76}$$

The expressions of the internal efforts $\boldsymbol{N}$ and moments $\boldsymbol{M}$ evaluated at the middle point are

$$\begin{aligned}\boldsymbol{N}_{n+\frac{1}{2}} &= \frac{1}{2}(\boldsymbol{N}_{n+1} + \boldsymbol{N}_n) \\ &= \frac{\boldsymbol{C}^N\boldsymbol{R}^{\mathrm{T}}_E}{4L}[(\boldsymbol{R}^{\mathrm{T}}_{An+1} + \boldsymbol{R}^{\mathrm{T}}_{Bn+1})\boldsymbol{x}_{ABn+1} + (\boldsymbol{R}^{\mathrm{T}}_{An} + \boldsymbol{R}^{\mathrm{T}}_{Bn})\boldsymbol{x}_{ABn}] - \boldsymbol{C}^N\boldsymbol{i}_1\end{aligned} \tag{77}$$

$$\boldsymbol{M}_{n+\frac{1}{2}} = \frac{1}{2}(\boldsymbol{M}_{n+1} + \boldsymbol{M}_n) = \frac{\boldsymbol{C}^M\boldsymbol{R}^{\mathrm{T}}_E}{2L}\mathrm{vect}(\boldsymbol{R}^{\mathrm{T}}_{An+1}\boldsymbol{R}_{Bn+1} + \boldsymbol{R}^{\mathrm{T}}_{An}\boldsymbol{R}_{Bn} - 2\boldsymbol{I}) \tag{78}$$

with the corresponding variations

$$\begin{aligned}\delta\boldsymbol{N}_{n+\frac{1}{2}} = \frac{\boldsymbol{C}^N\boldsymbol{R}^{\mathrm{T}}_E}{4L}\Big[&(\boldsymbol{R}^{\mathrm{T}}_{An+1}\widetilde{\boldsymbol{x}}_{ABn+1})\,\boldsymbol{T}_A\delta\boldsymbol{e}_A \\ &+(\boldsymbol{R}^{\mathrm{T}}_{Bn+1}\widetilde{\boldsymbol{x}}_{ABn+1})\,\boldsymbol{T}_B\delta\boldsymbol{e}_B + (\boldsymbol{R}^{\mathrm{T}}_{An+1} + \boldsymbol{R}^{\mathrm{T}}_{Bn+1})(2\delta\boldsymbol{u}_{Bn+\frac{1}{2}} - 2\delta\boldsymbol{u}_{An+\frac{1}{2}})\Big]\end{aligned} \tag{79}$$

with

$$\boldsymbol{C}^N = \mathrm{diag}(\,EA \quad GA_2 \quad GA_3\,), \quad \boldsymbol{C}^M = \mathrm{diag}(\,GJ \quad EI_2 \quad EI_3\,) \tag{80}$$

$$\begin{aligned}\delta\boldsymbol{M}_{n+\frac{1}{2}} &= \frac{\boldsymbol{C}^M\boldsymbol{R}^{\mathrm{T}}_E}{2L}\mathrm{vect}(\boldsymbol{R}^{\mathrm{T}}_{An+1}\delta\boldsymbol{R}_{Bn+1} + \delta\boldsymbol{R}^{\mathrm{T}}_{An+1}\boldsymbol{R}_{Bn+1}) \\ &= \frac{\boldsymbol{C}^M\boldsymbol{R}^{\mathrm{T}}_E}{2L}\mathrm{vect}(\boldsymbol{R}^{\mathrm{T}}_{An+1}\boldsymbol{R}_{Bn+1}\delta\widetilde{\boldsymbol{\Theta}}_B - \delta\widetilde{\boldsymbol{\Theta}}_A\boldsymbol{R}^{\mathrm{T}}_{An+1}\boldsymbol{R}_{Bn+1}) \\ &= \frac{\boldsymbol{C}^M\boldsymbol{R}^{\mathrm{T}}_E}{2L}\left[\frac{1}{2}\overline{\mathrm{dev}}[\boldsymbol{R}^{\mathrm{T}}_{An+1}\boldsymbol{R}_{Bn+1}]\,\boldsymbol{T}_A\delta\boldsymbol{e}_A\right. \\ &\quad \left.-\frac{1}{2}\overline{\mathrm{dev}}[\boldsymbol{R}^{\mathrm{T}}_{Bn+1}\boldsymbol{R}_{An+1}]\,\boldsymbol{T}_B\delta\boldsymbol{e}_B\right]\end{aligned} \tag{81}$$

where

$$\begin{aligned}\boldsymbol{x}_{ABn} &= (\boldsymbol{E}_1 L + \boldsymbol{u}_{Bn} - \boldsymbol{u}_{An}) \\ \boldsymbol{x}_{ABn+1} &= (\boldsymbol{E}_1 L + \boldsymbol{u}_{Bn+1} - \boldsymbol{u}_{An+1})\end{aligned} \tag{82}$$

In order to arrive to the expression of $\boldsymbol{B}_{n+\frac{1}{2}}$, we will use the approximation $\boldsymbol{R}_{0.5} \simeq \frac{\boldsymbol{R}_A + \boldsymbol{R}_B}{2}$ in the computation of the axial strains giving

$$\boldsymbol{\Gamma}_{0.5} = \boldsymbol{R}_E^{\mathrm{T}} \frac{\boldsymbol{R}_A^{\mathrm{T}} + \boldsymbol{R}_B^{\mathrm{T}}}{2} \left(\boldsymbol{E}_1 + \frac{\boldsymbol{u}_B - \boldsymbol{u}_A}{L} \right) - \boldsymbol{i}_1 \tag{83}$$

Note that the *increment* in average rotations between the initial and final time instants may be written

$$\begin{aligned} 2\overline{\Delta}\boldsymbol{R} &= 2(\boldsymbol{R}_{n+1} - \boldsymbol{R}_n) \\ &= (\boldsymbol{R}_{An+1} - \boldsymbol{R}_{An}) + (\boldsymbol{R}_{Bn+1} - \boldsymbol{R}_{Bn}) \\ &= \boldsymbol{R}_{An+\frac{1}{2}}(\boldsymbol{F}_A - \boldsymbol{F}_A^{\mathrm{T}}) + \boldsymbol{R}_{Bn+\frac{1}{2}}(\boldsymbol{F}_B - \boldsymbol{F}_B^{\mathrm{T}}) \\ &= \boldsymbol{R}_{An}\boldsymbol{F}_A \overline{\Delta}\widetilde{\boldsymbol{\Theta}}_A + \boldsymbol{R}_{Bn}\boldsymbol{F}_B \overline{\Delta}\widetilde{\boldsymbol{\Theta}}_B \end{aligned} \tag{84}$$

where we use the notation

$$\overline{\Delta}(\bullet) = (\bullet)_{n+1} - (\bullet)_n \tag{85}$$

to indicate the difference from quantities at time t_{n+1} with respect to quantities at time t_n.

Note also that the *mean* average rotation between the initial and final time instants results

$$\begin{aligned} \frac{\boldsymbol{R}_{n+1} + \boldsymbol{R}_n}{2} &= \frac{1}{4}(\boldsymbol{R}_{An+1} + \boldsymbol{R}_{An} + \boldsymbol{R}_{Bn+1} + \boldsymbol{R}_{Bn}) \\ &= \frac{1}{2}\left(\boldsymbol{R}_{An+\frac{1}{2}}^{\mathrm{T}} + \boldsymbol{R}_{Bn+\frac{1}{2}}^{\mathrm{T}} \right) \end{aligned} \tag{86}$$

Finally, using Eqs. (83)–(86), we get the *identity*

$$\begin{aligned} \boldsymbol{\Gamma}_{n+1} - \boldsymbol{\Gamma}_n = {} & \frac{\boldsymbol{R}_E^{\mathrm{T}}}{2L}\left(-\overline{\Delta}\widetilde{\boldsymbol{\Theta}}_A \boldsymbol{R}_{An+\frac{1}{2}}^{\mathrm{T}} - \overline{\Delta}\widetilde{\boldsymbol{\Theta}}_B \boldsymbol{R}_{Bn+\frac{1}{2}}^{\mathrm{T}} \right) \boldsymbol{x}_{ABn+\frac{1}{2}} \\ & + \frac{\boldsymbol{R}_E^{\mathrm{T}}}{2L}\left(\boldsymbol{R}_{An+\frac{1}{2}}^{\mathrm{T}} + \boldsymbol{R}_{Bn+\frac{1}{2}}^{\mathrm{T}} \right)(\overline{\Delta}\boldsymbol{u}_B - \overline{\Delta}\boldsymbol{u}_A) \\ = {} & -\frac{\boldsymbol{R}_E^{\mathrm{T}}}{2L}\left[\boldsymbol{R}_{An+\frac{1}{2}}^{\mathrm{T}} + \boldsymbol{R}_{Bn+\frac{1}{2}}^{\mathrm{T}} \right](\overline{\Delta}\boldsymbol{u}_A - \overline{\Delta}\boldsymbol{u}_B) \\ & + \frac{\boldsymbol{R}_E^{\mathrm{T}}}{2L}\left[\left(\widetilde{\boldsymbol{R}_{An+\frac{1}{2}}^{\mathrm{T}} \boldsymbol{x}_{ABn+\frac{1}{2}}} \right)\overline{\Delta}\boldsymbol{\Theta}_A + \left(\widetilde{\boldsymbol{R}_{Bn+\frac{1}{2}}^{\mathrm{T}} \boldsymbol{x}_{ABn+\frac{1}{2}}} \right)\overline{\Delta}\boldsymbol{\Theta}_B \right] \end{aligned} \tag{87}$$

where

$$\boldsymbol{x}_{ABn+\frac{1}{2}} = \left(\boldsymbol{E}_1 L + \boldsymbol{u}_{Bn+\frac{1}{2}} - \boldsymbol{u}_{An+\frac{1}{2}} \right) \tag{88}$$

After truncation of the exponential series $\boldsymbol{H} = \exp(\widetilde{\boldsymbol{\phi}}) = \boldsymbol{I} + \widetilde{\boldsymbol{\phi}} + \cdots$ to first order, we may approximate the skew of $\boldsymbol{\phi}$ in the form

$$\widetilde{\boldsymbol{\phi}} \simeq \sqrt{\boldsymbol{R}_A^{\mathrm{T}}\boldsymbol{R}_B} - \boldsymbol{I} \simeq \frac{1}{2}(\boldsymbol{R}_A^{\mathrm{T}}\boldsymbol{R}_B - \boldsymbol{I}) \tag{89}$$

By using the latter expression into Eq. (14), we get the following approximation for the curvatures vector at the midpoint of the beam which is suitable for implementation of the energy conserving time integration algorithm

$$\boldsymbol{K}_{0.5} = \frac{\boldsymbol{R}_E^{\mathrm{T}}}{L}\,\mathrm{vect}(\boldsymbol{R}_A^{\mathrm{T}}\boldsymbol{R}_B - \boldsymbol{I}) \tag{90}$$

Indeed, the time increment of the curvatures at the midpoint of the beam may be written

$$\boldsymbol{K}_{n+1} - \boldsymbol{K}_n = \frac{\boldsymbol{R}_E^{\mathrm{T}}}{L}\,\mathrm{vect}(\boldsymbol{R}_{An+1}^{\mathrm{T}}\boldsymbol{R}_{Bn+1} - \boldsymbol{R}_{An}^{\mathrm{T}}\boldsymbol{R}_{Bn}) \tag{91}$$

The term between parentheses on the RHS may be transformed giving

$$\begin{aligned} & \boldsymbol{R}_{An+1}^{\mathrm{T}}\boldsymbol{R}_{Bn+1} - \boldsymbol{R}_{An}^{\mathrm{T}}\boldsymbol{R}_{Bn} \\ & \quad = \boldsymbol{R}_{An+1}^{\mathrm{T}}\boldsymbol{R}_{Bn+1} - \boldsymbol{R}_{An}^{\mathrm{T}}\boldsymbol{R}_{Bn+1} + \boldsymbol{R}_{An}^{\mathrm{T}}\boldsymbol{R}_{Bn+1} - \boldsymbol{R}_{An}^{\mathrm{T}}\boldsymbol{R}_{Bn} \\ & \quad = (\boldsymbol{F}_A^{\mathrm{T}} - \boldsymbol{F}_A)\boldsymbol{R}_{An+\frac{1}{2}}^{\mathrm{T}}\boldsymbol{R}_{Bn+\frac{1}{2}}\boldsymbol{F}_B - \boldsymbol{F}_A\boldsymbol{R}_{An+\frac{1}{2}}^{\mathrm{T}}\boldsymbol{R}_{Bn+\frac{1}{2}}(\boldsymbol{F}_B^{\mathrm{T}} - \boldsymbol{F}_B) \\ & \quad = -\overline{\Delta}\widetilde{\boldsymbol{\Theta}}_A\boldsymbol{R}_{An+\frac{1}{2}}^{\mathrm{T}}\boldsymbol{R}_{Bn+1} + \boldsymbol{R}_{An}^{\mathrm{T}}\boldsymbol{R}_{Bn+\frac{1}{2}}\overline{\Delta}\widetilde{\boldsymbol{\Theta}}_B \\ & \quad = -\overline{\Delta}\widetilde{\boldsymbol{\Theta}}_A\boldsymbol{P}_A + \boldsymbol{P}_B\overline{\Delta}\widetilde{\boldsymbol{\Theta}}_B \end{aligned} \tag{92}$$

with $\boldsymbol{P}_A = \boldsymbol{R}_{An+\frac{1}{2}}^{\mathrm{T}}\boldsymbol{R}_{Bn+\frac{1}{2}}\boldsymbol{F}_B$ and $\boldsymbol{P}_B = \boldsymbol{F}_A\boldsymbol{R}_{An+\frac{1}{2}}^{\mathrm{T}}\boldsymbol{R}_{Bn+\frac{1}{2}}$. After some algebraic steps, we can verify that

$$\begin{aligned} \mathrm{vect}(-\overline{\Delta}\widetilde{\boldsymbol{\Theta}}_A\boldsymbol{P}_A + \boldsymbol{P}_B\overline{\Delta}\widetilde{\boldsymbol{\Theta}}_B) = {} & \frac{1}{2}\left(\boldsymbol{P}_B^{\mathrm{T}} + \mathrm{tr}(\boldsymbol{P}_B^{\mathrm{T}})\boldsymbol{I}\right)\overline{\Delta}\boldsymbol{\Theta}_B \\ & - \frac{1}{2}(\boldsymbol{P}_A + \mathrm{tr}(\boldsymbol{P}_A)\boldsymbol{I})\overline{\Delta}\boldsymbol{\Theta}_A \end{aligned} \tag{93}$$

and therefore, the curvatures time increment is written

$$\boldsymbol{K}_{n+1} - \boldsymbol{K}_n = \frac{\boldsymbol{R}_E^{\mathrm{T}}}{2L}\overline{\mathrm{dev}}[\boldsymbol{P}_A]\overline{\Delta}\boldsymbol{\Theta}_A - \frac{\boldsymbol{R}_E^{\mathrm{T}}}{2L}\overline{\mathrm{dev}}[\boldsymbol{P}_B^{\mathrm{T}}]\overline{\Delta}\boldsymbol{\Theta}_B \tag{94}$$

Finally, using Eqs. (87) and (94), we get

$$\begin{pmatrix} \overline{\Delta}\boldsymbol{\Gamma} \\ \overline{\Delta}\boldsymbol{K} \end{pmatrix} = \boldsymbol{B}_{n+\frac{1}{2}}\overline{\Delta}\boldsymbol{q} = \boldsymbol{B}_{n+\frac{1}{2}} \begin{pmatrix} \overline{\Delta}\boldsymbol{u}_A \\ \overline{\Delta}\boldsymbol{\Theta}_A \\ \overline{\Delta}\boldsymbol{u}_B \\ \overline{\Delta}\boldsymbol{\Theta}_B \end{pmatrix} \tag{95}$$

where

$$\boldsymbol{B}_{n+\frac{1}{2}}^{\mathrm{T}} = \frac{1}{2L} \begin{pmatrix} -\left[\boldsymbol{R}_{An+\frac{1}{2}} + \boldsymbol{R}_{Bn+\frac{1}{2}} \right]\boldsymbol{R}_E & 0 \\ -\left[\widetilde{\boldsymbol{R}_{An+\frac{1}{2}}^{\mathrm{T}}\boldsymbol{x}_{ABn+\frac{1}{2}}} \right]\boldsymbol{R}_E & \overline{\mathrm{dev}}[\boldsymbol{P}_A^{\mathrm{T}}]\boldsymbol{R}_E \\ \left[\boldsymbol{R}_{An+\frac{1}{2}} + \boldsymbol{R}_{Bn+\frac{1}{2}} \right]\boldsymbol{R}_E & 0 \\ -\left[\widetilde{\boldsymbol{R}_{Bn+\frac{1}{2}}^{\mathrm{T}}\boldsymbol{x}_{ABn+\frac{1}{2}}} \right]\boldsymbol{R}_E & -\overline{\mathrm{dev}}[\boldsymbol{P}_B]\boldsymbol{R}_E \end{pmatrix} \tag{96}$$

After replacement into Eq. (76), we obtain the expression of the averaged internal forces

$$\boldsymbol{F}^*_{\mathrm{int}_{n+\frac{1}{2}}} = \begin{pmatrix} -\frac{1}{2}\left[\boldsymbol{R}_{An+\frac{1}{2}} + \boldsymbol{R}_{Bn+\frac{1}{2}} \right]\boldsymbol{N}^E_{n+\frac{1}{2}} \\ -\frac{1}{2}\left[\widetilde{\boldsymbol{R}_{An+\frac{1}{2}}^{\mathrm{T}}\boldsymbol{x}_{ABn+\frac{1}{2}}} \right]\boldsymbol{N}^E_{n+\frac{1}{2}} + \frac{1}{2}\overline{\mathrm{dev}}[\boldsymbol{P}_A^{\mathrm{T}}]\boldsymbol{M}^E_{n+\frac{1}{2}} \\ \frac{1}{2}\left[\boldsymbol{R}_{An+\frac{1}{2}} + \boldsymbol{R}_{Bn+\frac{1}{2}} \right]\boldsymbol{N}^E_{n+\frac{1}{2}} \\ -\frac{1}{2}\left[\widetilde{\boldsymbol{R}_{Bn+\frac{1}{2}}^{\mathrm{T}}\boldsymbol{x}_{ABn+\frac{1}{2}}} \right]\boldsymbol{N}^E_{n+\frac{1}{2}} - \frac{1}{2}\overline{\mathrm{dev}}[\boldsymbol{P}_B]\boldsymbol{M}^E_{n+\frac{1}{2}} \end{pmatrix} \tag{97}$$

where

$$\begin{aligned} \boldsymbol{M}^E_{n+\frac{1}{2}} &= \boldsymbol{R}_E\boldsymbol{M}_{n+\frac{1}{2}} \\ \boldsymbol{N}^E_{n+\frac{1}{2}} &= \boldsymbol{R}_E\boldsymbol{N}_{n+\frac{1}{2}} \end{aligned} \tag{98}$$

We may see, by comparing with Eq. (57), the time averaged character of the internal forces vector $\boldsymbol{F}^*_{\mathrm{int}_{n+\frac{1}{2}}}$.

The tangent stiffness matrix $\boldsymbol{S}^*$ is obtained by differentiation of the internal forces vector, as we did previously in Section 2.5. It is worth noting that in this case the stiffness

is not symmetric, which is characteristic of the energy conserving algorithm.

The tangent stiffness matrix has the following expression:

$$\boldsymbol{S}^* = \begin{bmatrix} \boldsymbol{S}^*_{11} & \boldsymbol{S}^*_{12} & \boldsymbol{S}^*_{13} & \boldsymbol{S}^*_{14} \\ \boldsymbol{S}^*_{21} & \boldsymbol{S}^*_{22} & \boldsymbol{S}^*_{23} & \boldsymbol{S}^*_{24} \\ \boldsymbol{S}^*_{31} & \boldsymbol{S}^*_{32} & \boldsymbol{S}^*_{33} & \boldsymbol{S}^*_{34} \\ \boldsymbol{S}^*_{41} & \boldsymbol{S}^*_{42} & \boldsymbol{S}^*_{43} & \boldsymbol{S}^*_{44} \end{bmatrix} \tag{99}$$

The corresponding terms $\boldsymbol{S}^*_{ii}$ are

$$\boldsymbol{S}^*_{11} = 4\left[\boldsymbol{R}_{An+\frac{1}{2}} + \boldsymbol{R}_{Bn+\frac{1}{2}}\right]\boldsymbol{C}^{NE}[\boldsymbol{R}^{\mathrm{T}}_{An+1} + \boldsymbol{R}^{\mathrm{T}}_{Bn+1}]$$

$$\boldsymbol{S}^*_{12} = \frac{1}{4}\boldsymbol{R}_{An+1}\widetilde{\boldsymbol{N}^E_{n+\frac{1}{2}}}\boldsymbol{T}_A(\boldsymbol{e}) - 2\left[\boldsymbol{R}_{An+\frac{1}{2}} + \boldsymbol{R}_{Bn+\frac{1}{2}}\right]\boldsymbol{C}^{NE}\left[\boldsymbol{R}^{\mathrm{T}}_{An+1}\widetilde{\boldsymbol{x}_{ABn+1}}\right]\boldsymbol{T}_A(\boldsymbol{e})$$

$$\boldsymbol{S}^*_{13} = -\boldsymbol{S}^*_{11}$$

$$\boldsymbol{S}^*_{14} = \frac{1}{4}\boldsymbol{R}_{Bn+1}\widetilde{\boldsymbol{N}^E_{n+\frac{1}{2}}}\boldsymbol{T}_B(\boldsymbol{e}) - 2\left[\boldsymbol{R}_{An+\frac{1}{2}} + \boldsymbol{R}_{Bn+\frac{1}{2}}\right]\boldsymbol{C}^{NE}[\boldsymbol{R}^{\mathrm{T}}_{Bn+1}\widetilde{\boldsymbol{x}_{ABn+1}}]\boldsymbol{T}_B(\boldsymbol{e})$$

$$\boldsymbol{S}^*_{21} = 4\left[\widetilde{\boldsymbol{R}^{\mathrm{T}}_{An+\frac{1}{2}}\boldsymbol{x}_{ABn+\frac{1}{2}}}\right]\boldsymbol{C}^{NE}[\boldsymbol{R}^{\mathrm{T}}_{An+1} + \boldsymbol{R}^{\mathrm{T}}_{Bn+1}] - \frac{1}{2}\widetilde{\boldsymbol{N}^E_{n+\frac{1}{2}}}\boldsymbol{R}^{\mathrm{T}}_{An+\frac{1}{2}}$$

$$\boldsymbol{S}^*_{22} = \frac{1}{2}\widetilde{\boldsymbol{N}^E_{n+\frac{1}{2}}}\boldsymbol{D}^{\mathrm{T}}_{Ax} - 2\left[\widetilde{\boldsymbol{R}^{\mathrm{T}}_{An+\frac{1}{2}}\boldsymbol{x}_{ABn+\frac{1}{2}}}\right]\boldsymbol{C}^{NE}\left[\boldsymbol{R}^{\mathrm{T}}_{An+1}\widetilde{\boldsymbol{x}_{ABn+1}}\right]\boldsymbol{T}_A(\boldsymbol{e}) + 2\,\overline{\mathrm{dev}}[\boldsymbol{P}^{\mathrm{T}}_A]\boldsymbol{C}^{ME}\overline{\mathrm{dev}}[\boldsymbol{R}^{\mathrm{T}}_{An+1}\boldsymbol{R}_{Bn+1}]\boldsymbol{T}_A(\boldsymbol{e}) + \frac{1}{2}\boldsymbol{R}^{\mathrm{T}}_{Bn+1}\boldsymbol{R}_{An}\boldsymbol{D}_{AM} - \frac{1}{2}\boldsymbol{w}_A\left[\boldsymbol{M}^E_{n+\frac{1}{2}}\right]^{\mathrm{T}}$$

$$\boldsymbol{S}^*_{23} = -\boldsymbol{S}^*_{21}$$

$$\boldsymbol{S}^*_{24} = -2\left[\widetilde{\boldsymbol{R}^{\mathrm{T}}_{An+\frac{1}{2}}\boldsymbol{x}_{ABn+\frac{1}{2}}}\right]\boldsymbol{C}^{NE}[\boldsymbol{R}^{\mathrm{T}}_{Bn+1}\widetilde{\boldsymbol{x}_{ABn+1}}]\boldsymbol{T}_B(\boldsymbol{e}) + \frac{1}{2}\left[\boldsymbol{P}^{\mathrm{T}}_A\widetilde{\boldsymbol{M}^E_{n+\frac{1}{2}}}\right]\boldsymbol{T}_B(\boldsymbol{e}) + \boldsymbol{M}^E_{n+\frac{1}{2}}[\mathrm{vect}(\boldsymbol{P}_A)]^{\mathrm{T}}\boldsymbol{T}_B(\boldsymbol{e}) - 2\overline{\mathrm{dev}}[\boldsymbol{P}^{\mathrm{T}}_A]\boldsymbol{C}^{ME}[\overline{\mathrm{dev}}[\boldsymbol{R}^{\mathrm{T}}_{Bn+1}\boldsymbol{R}_{An+1}]]\boldsymbol{T}_B(\boldsymbol{e})$$

$$\boldsymbol{S}^*_{31} = -\boldsymbol{S}^*_{11}$$

$$\boldsymbol{S}^*_{32} = -\boldsymbol{S}^*_{12}$$

$$\boldsymbol{S}^*_{33} = \boldsymbol{S}^*_{11}$$

$$\boldsymbol{S}^*_{34} = -\boldsymbol{S}^*_{14}$$

$$\boldsymbol{S}^*_{41} = 4\left[\widetilde{\boldsymbol{R}^{\mathrm{T}}_{Bn+\frac{1}{2}}\boldsymbol{x}_{ABn+\frac{1}{2}}}\right]\boldsymbol{C}^{NE}[\boldsymbol{R}^{\mathrm{T}}_{An+1} + \boldsymbol{R}^{\mathrm{T}}_{Bn+1}] - \frac{1}{2}\widetilde{\boldsymbol{N}^E_{n+\frac{1}{2}}}\boldsymbol{R}^{\mathrm{T}}_{Bn+\frac{1}{2}}$$

$$\boldsymbol{S}^*_{42} = -2\left[\widetilde{\boldsymbol{R}^{\mathrm{T}}_{Bn+\frac{1}{2}}\boldsymbol{x}_{ABn+\frac{1}{2}}}\right]\boldsymbol{C}^{NE}[\boldsymbol{R}^{\mathrm{T}}_{An+1}\widetilde{\boldsymbol{x}_{ABn+1}}]\boldsymbol{T}_A(\boldsymbol{e}) - 2\,\overline{\mathrm{dev}}[\boldsymbol{P}_B]\boldsymbol{C}^{ME}\overline{\mathrm{dev}}[\boldsymbol{R}^{\mathrm{T}}_{An+1}\boldsymbol{R}_{Bn+1}]\boldsymbol{T}_A(\boldsymbol{e})$$

$$\boldsymbol{S}^*_{43} = -\boldsymbol{S}^*_{41}$$

$$\boldsymbol{S}^*_{44} = -2\left[\widetilde{\boldsymbol{R}^{\mathrm{T}}_{Bn+\frac{1}{2}}\boldsymbol{x}_{ABn+\frac{1}{2}}}\right]\boldsymbol{C}^{NE}[\boldsymbol{R}^{\mathrm{T}}_{Bn+1}\widetilde{\boldsymbol{x}_{ABn+1}}]\boldsymbol{T}_B(\boldsymbol{e}) + \frac{1}{2}\widetilde{\boldsymbol{N}^E_{n+\frac{1}{2}}}\boldsymbol{D}^{\mathrm{T}}_{Bx} - \frac{1}{2}\boldsymbol{R}^{\mathrm{T}}_{An}\boldsymbol{R}_{Bn}\boldsymbol{D}_{BM} - \frac{1}{2}\boldsymbol{w}_B\left(\boldsymbol{M}^E_{n+\frac{1}{2}}\right)^{\mathrm{T}} + 2\overline{\mathrm{dev}}[\boldsymbol{P}_B]\boldsymbol{C}^{ME}\overline{\mathrm{dev}}[\boldsymbol{R}^{\mathrm{T}}_{Bn+1}\boldsymbol{R}_{An+1}]\boldsymbol{T}_B(\boldsymbol{e})$$

where

$$\boldsymbol{D}_{AM} = -\frac{1}{e_{A0}}\boldsymbol{M}^E_{n+\frac{1}{2}}\boldsymbol{e}^{\mathrm{T}}_A + \frac{\boldsymbol{e}^{\mathrm{T}}_A\boldsymbol{M}^E_{n+\frac{1}{2}}}{e_{A0}(1+e_{A0})^2}\boldsymbol{e}_A\boldsymbol{e}^{\mathrm{T}}_A - \widetilde{\boldsymbol{M}^E_{n+\frac{1}{2}}} + \boldsymbol{e}^{\mathrm{T}}_A\boldsymbol{M}^E_{n+\frac{1}{2}}\boldsymbol{I} + \frac{1}{1+e_{A0}}\boldsymbol{e}_A(\boldsymbol{M}^E_{n+\frac{1}{2}})^{\mathrm{T}}$$

$$\boldsymbol{D}_{BM} = -\frac{1}{e_{B0}}\boldsymbol{M}^E_{n+\frac{1}{2}}\boldsymbol{e}^{\mathrm{T}}_B + \frac{\boldsymbol{e}^{\mathrm{T}}_B\boldsymbol{M}^E_{n+\frac{1}{2}}}{e_{B0}(1+e_{B0})^2}\boldsymbol{e}_B\boldsymbol{e}^{\mathrm{T}}_B - \widetilde{\boldsymbol{M}^E_{n+\frac{1}{2}}} + \boldsymbol{e}^{\mathrm{T}}_B\boldsymbol{M}^E_{n+\frac{1}{2}}\boldsymbol{I} + \frac{1}{1+e_{B0}}\boldsymbol{e}_B\left(\boldsymbol{M}^E_{n+\frac{1}{2}}\right)^{\mathrm{T}}$$

$$\boldsymbol{D}^{\mathrm{T}}_{Ax} = -\frac{1}{e_{A0}}\left(\boldsymbol{R}^{\mathrm{T}}_{An}\boldsymbol{x}_{ABn+\frac{1}{2}}\right)\boldsymbol{e}^{\mathrm{T}}_A + \frac{\boldsymbol{e}^{\mathrm{T}}_A\left(\boldsymbol{R}^{\mathrm{T}}_{An}\boldsymbol{x}_{ABn+\frac{1}{2}}\right)}{e_{A0}(1+e_{A0})^2}\boldsymbol{e}_A\boldsymbol{e}^{\mathrm{T}}_A + \left(\widetilde{\boldsymbol{R}^{\mathrm{T}}_{An}\boldsymbol{x}_{ABn+\frac{1}{2}}}\right) + \frac{1}{1+e_{A0}}\boldsymbol{e}_A\left(\boldsymbol{R}^{\mathrm{T}}_{An}\boldsymbol{x}_{ABn+\frac{1}{2}}\right)^{\mathrm{T}} + \boldsymbol{e}^{\mathrm{T}}_A\left(\boldsymbol{R}^{\mathrm{T}}_{An}\boldsymbol{x}_{ABn+\frac{1}{2}}\right)\boldsymbol{I}$$

$$\boldsymbol{D}^{\mathrm{T}}_{Bx} = -\frac{1}{e_{B0}}\left(\boldsymbol{R}^{\mathrm{T}}_{Bn}\boldsymbol{x}_{ABn+\frac{1}{2}}\right)\boldsymbol{e}^{\mathrm{T}}_B + \frac{\boldsymbol{e}^{\mathrm{T}}_B\left(\boldsymbol{R}^{\mathrm{T}}_{Bn}\boldsymbol{x}_{ABn+\frac{1}{2}}\right)}{e_{B0}(1+e_{B0})^2}\boldsymbol{e}_B\boldsymbol{e}^{\mathrm{T}}_B + \left(\widetilde{\boldsymbol{R}^{\mathrm{T}}_{Bn}\boldsymbol{x}_{ABn+\frac{1}{2}}}\right) + \frac{1}{1+e_{B0}}\boldsymbol{e}_B\left(\boldsymbol{R}^{\mathrm{T}}_{Bn}\boldsymbol{x}_{ABn+\frac{1}{2}}\right)^{\mathrm{T}} + \boldsymbol{e}^{\mathrm{T}}_B\left(\boldsymbol{R}^{\mathrm{T}}_{Bn}\boldsymbol{x}_{ABn+\frac{1}{2}}\right)\boldsymbol{I}$$

$$\boldsymbol{C}^{NE} = \frac{\boldsymbol{R}_E\boldsymbol{C}^N\boldsymbol{R}^{\mathrm{T}}_E}{16L}$$

$$\boldsymbol{C}^{ME} = \frac{\boldsymbol{R}_E\boldsymbol{C}^M\boldsymbol{R}^{\mathrm{T}}_E}{16L}$$

$$\boldsymbol{w}_A = \frac{\mathrm{d}}{\mathrm{d}\boldsymbol{e}_A}\mathrm{tr}(\boldsymbol{R}^{\mathrm{T}}_{Bn+1}\boldsymbol{R}_{An}\boldsymbol{F}_A)$$

$$\boldsymbol{w}_B = \frac{\mathrm{d}}{\mathrm{d}\boldsymbol{e}_B}\mathrm{tr}(\boldsymbol{R}^{\mathrm{T}}_{An}\boldsymbol{R}_{Bn}\boldsymbol{F}_B)$$

3.3. Energy preservation

To demonstrate the energy preservation of the formulation, we have to prove the nullity of the virtual work of inertia and internal discrete forces of the beam when there are no external forces acting on the system. In order to do that, we pre-multiply the discrete expressions of $\boldsymbol{F}^*_{\mathrm{int}_{n+\frac{1}{2}}}$ and $\boldsymbol{F}_{\mathrm{iner}_{n+\frac{1}{2}}}$ by the displacements jump $\Delta\boldsymbol{q}$

$$\Delta\mathscr{W}_{\mathrm{int}} + \Delta\mathscr{W}_{\mathrm{iner}} = \Delta\boldsymbol{q}^{\mathrm{T}}\boldsymbol{F}^*_{\mathrm{int}_{n+\frac{1}{2}}} + \Delta\boldsymbol{q}^{\mathrm{T}}\boldsymbol{F}_{\mathrm{iner}_{n+\frac{1}{2}}} = 0 \tag{100}$$

where the internal forces at the mid-point $\boldsymbol{F}^*_{\mathrm{int}_{n+\frac{1}{2}}}$ were computed in the averaged form of Eq. (76) and verify

$$\mathscr{V}_{n+1} - \mathscr{V}_n = \Delta\boldsymbol{q}^{\mathrm{T}}\boldsymbol{F}^*_{\mathrm{int}_{n+\frac{1}{2}}} \tag{101}$$

It only remains to verify that the work done by the inertial forces over a time step is the jump of kinetic energy. In order to do that we pre-multiply first the expression (68) by Δq^{T}, obtaining

$$\Delta\boldsymbol{q}^{\mathrm{T}}\boldsymbol{M}_{n+\frac{1}{2}}\boldsymbol{a}_{n+\frac{1}{2}} = \frac{1}{h}\Delta\boldsymbol{q}^{\mathrm{T}}\boldsymbol{T}^{\mathrm{T}}_{n+\frac{1}{2}}\overline{\boldsymbol{M}}_{n+\frac{1}{2}}(\boldsymbol{v}_{n+1} - \boldsymbol{v}_n) \tag{102}$$

where

$$\overline{\boldsymbol{M}}_{n+\frac{1}{2}} = \int_0^L \boldsymbol{P}(s)^{\mathrm{T}}\begin{bmatrix} m\boldsymbol{I} & 0 \\ 0 & \boldsymbol{J} \end{bmatrix}\boldsymbol{P}(s)\mathrm{d}s \tag{103}$$

After some algebra we obtain that

$$\Delta \boldsymbol{q}^{\mathrm{T}} \boldsymbol{M}_{n+\frac{1}{2}} \boldsymbol{a}_{n+\frac{1}{2}} = \mathscr{K}_{n+1} - \mathscr{K}_n \tag{104}$$

being

$$\mathscr{K} = \frac{mL}{12}\left[\dot{\boldsymbol{x}}_A^{\mathrm{T}}\left(2\dot{\boldsymbol{x}}_A^{\mathrm{T}} + \dot{\boldsymbol{x}}_B^{\mathrm{T}}\right) + \dot{\boldsymbol{x}}_B^{\mathrm{T}}\left(\dot{\boldsymbol{x}}_A^{\mathrm{T}} + 2\dot{\boldsymbol{x}}_B^{\mathrm{T}}\right)\right] + \frac{L}{12}\left[\boldsymbol{\Omega}_A^{\mathrm{T}}\boldsymbol{J}\left(2\boldsymbol{\Omega}_A^{\mathrm{T}} + \boldsymbol{\Omega}_B^{\mathrm{T}}\right) + \boldsymbol{\Omega}_B^{\mathrm{T}}\boldsymbol{J}\left(\boldsymbol{\Omega}_A^{\mathrm{T}} + \boldsymbol{\Omega}_B^{\mathrm{T}}\right)\right] \tag{105}$$

the kinetic energy expression for the beam element.

For the gyroscopic forces we have that

$$\Delta \boldsymbol{q}^{\mathrm{T}} \boldsymbol{F}_{\mathrm{gyro}_{n+\frac{1}{2}}} = \Delta \boldsymbol{q}^{\mathrm{T}} \boldsymbol{G}_{n+\frac{1}{2}} \dot{\boldsymbol{q}}_{n+\frac{1}{2}} = 0 \tag{106}$$

that become perfectly null due to the skew-symmetry of the matrix $\boldsymbol{G}_{n+\frac{1}{2}}$ (Eq. (71)).

4. Results and discussion

In this section we present several numerical simulations to show the behaviour of the new beam formulation.

The two first examples are intended to compare the performance of the element with results from the literature, verifying the exact conservation of the total energy of the system and the convergence rate of the algorithm.

The third and fourth examples are test cases of particular interest, since they involve solving the impact of beams with a rigid wall. These test cases, with a wide frequency spectrum excited both in axial and flexural deformation, could not be solved using conventional formulations based on the HHT time integration scheme [6,25].

4.1. Right-angle cantilever beam subject to out-of-plane loading

This test has been proposed in Ref. [26] where the authors use quadratic beam elements. Refs. [27,28] also took this example to compare their results. An L shape cantilever beam is set into motion by applying an out-of-plane concentrated load at its elbow as is depicted in Fig. 2. The applied force is linearly increasing on $0 \leqslant t \leqslant 1$ to reach the maximum value of 50 and then is decreasing on $1 \leqslant t \leqslant 2$ to reach the 0 value. In the remaining time until $t = 30$ the cantilever is undergoing free vibrations of finite amplitude with combined bending and torsion. Each leg of the L has a length of 10. Beam properties are $EA = 1 \times 10^6$, $EI = GJ = 1 \times 10^3$, $A_\rho = 1$ and $\boldsymbol{J}_\rho = \mathrm{diag}(20, 10, 10)$. The computations are carried out for a constant time step of $h = 0.125$, with finite element models using 10 and 20 elements. The computed response for out-of-plane displacements of the tip and the elbow are plotted in Figs. 3 and 4, respectively. Note that the beam is really subjected to very large displacements and rotations in 3D, being the amplitude of the vibration of the same order of the magnitude as the structure dimensions. We found a good agreement between our simulations and those of the literature [27,28,26]. A convergence

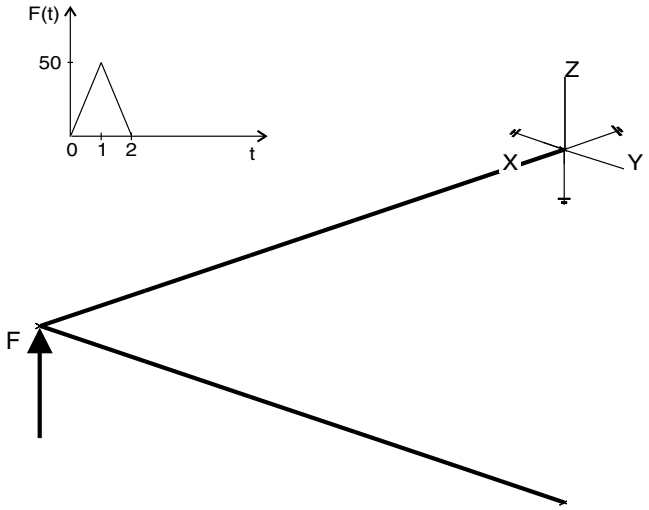

Fig. 2. Right-angle cantilever beam subject to out-of-plane loading.

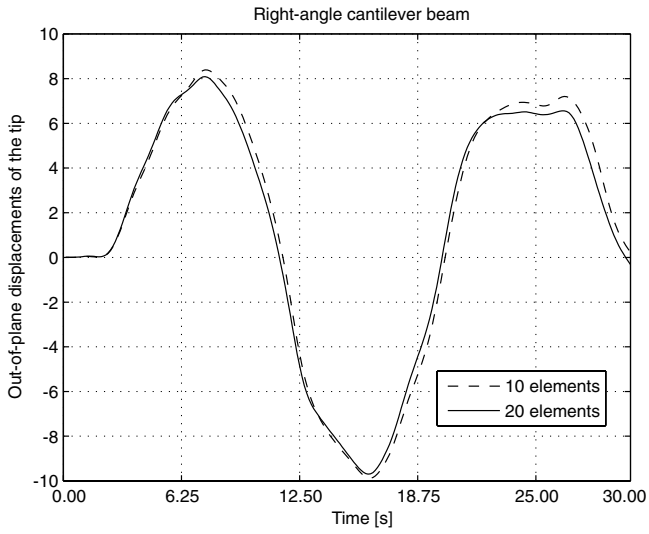

Fig. 3. Right-angle cantilever beam subject to out-of-plane loading: out-of-plane displacements of the tip for both models of 10 and 20 elements.

study of displacements is depicted in Fig. 5, where curves A and B provide the convergence rate for the beam formulation presented here, using the energy preserving scheme and the HHT scheme respectively. The curve C is obtained by using the beam model documented in Refs. [28,22]. Finally, Fig. 6 shows that total energy is perfectly conserved as it was expected.

4.2. Force driven flexible beam in a helicoidal motion

This example was presented by Ibrahimbegovic and Al Mikdad in Ref. [27] and deals with the helicoidal motion of a flexible straight beam initially placed in the horizontal plane (Fig. 7). One end of the beam is constrained to slide along the vertical axis and is subjected to a constant force $F = 4$ and a torque $M = 80$ applied both simultaneously during $0 \leqslant t \leqslant 2.5$. Computations are performed with the time step $h = 0.01$ for a finite element model that consists

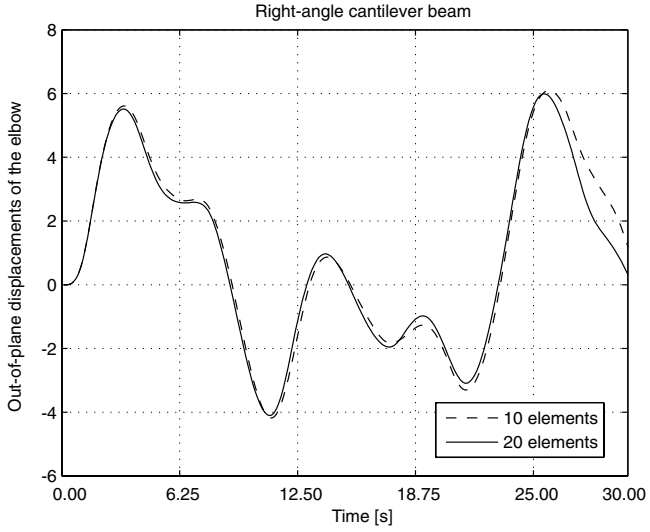

Fig. 4. Right-angle cantilever beam subject to out-of-plane loading: out-of-plane displacements of the elbow for both models of 10 and 20 elements.

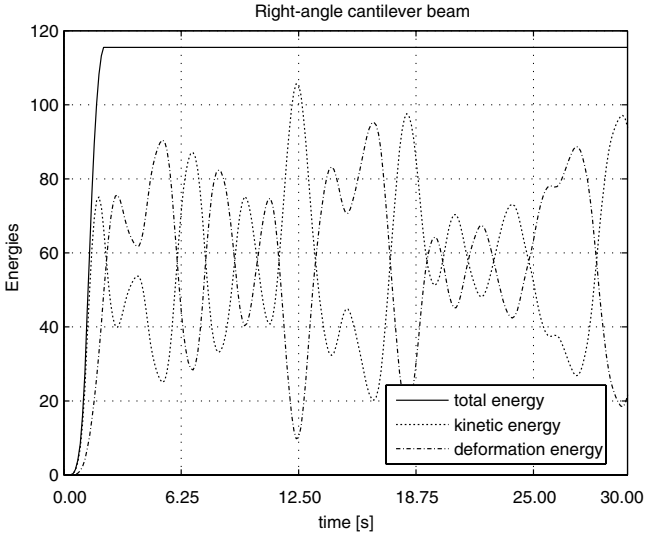

Fig. 6. Right-angle cantilever beam subject to out-of-plane loading: kinetic and deformation energies and energy preservation.

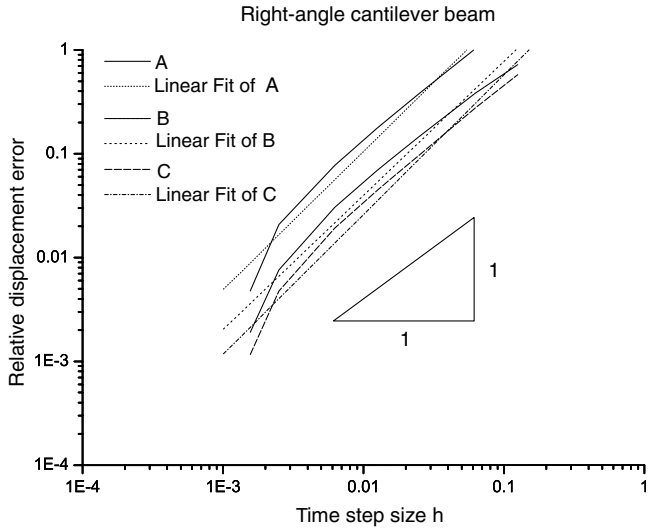

Fig. 5. Convergence rate for the analysis of a right-angle cantilever beam subject to out-of-plane loading for the new beam formulation introduced, using the energy preserving scheme (A) and the HHT scheme (B). Curve (C) was obtained using the beam model of [28,22] using HHT integration scheme.

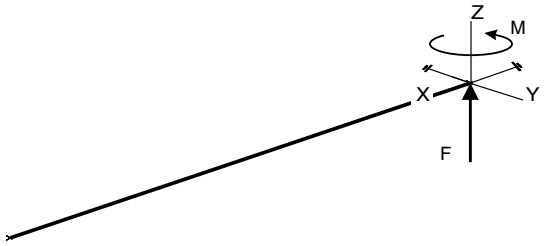

Fig. 7. Force driven flexible beam in a helicoidal motion.

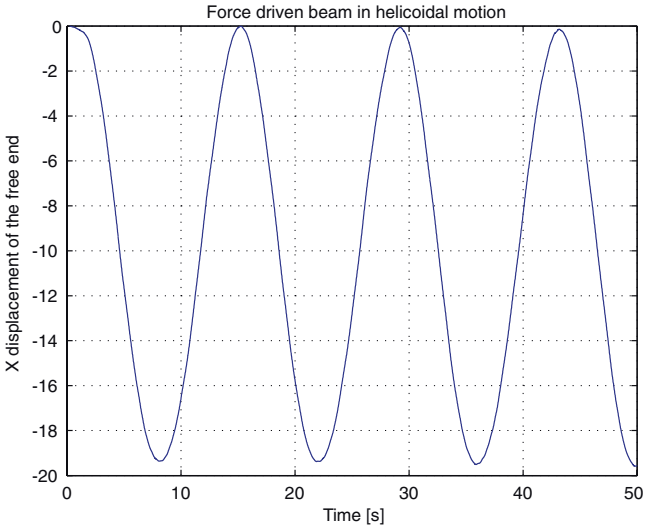

Fig. 8. Force driven flexible beam in a helicoidal motion: X-displacement of the free end.

of 10 beam elements. Beam properties are $EA = 1 \times 10^4$, $EI = GJ = 1 \times 10^3$, $A_\rho = 1$ and $\boldsymbol{J}_\rho = \mathrm{diag}(20, 10, 10)$.

The dynamic responses for displacement components of the free end are plotted in Figs. 8–10. Fig. 11 plots the total energy of the system. The results match with those of [27].

4.3. Two impact problems

The examples introduced in this section were chosen in order to emphasize the performance of the new beam formulation, by solving two problems that could not be solved with another more complex beam formulation that employed the HHT integration scheme [6,25].

4.3.1. Contact model

The point contact condition between two bodies can be expressed as an inequality $q \geqslant 0$. If the bodies are assumed to be deformable under hypothesis of small deformations,

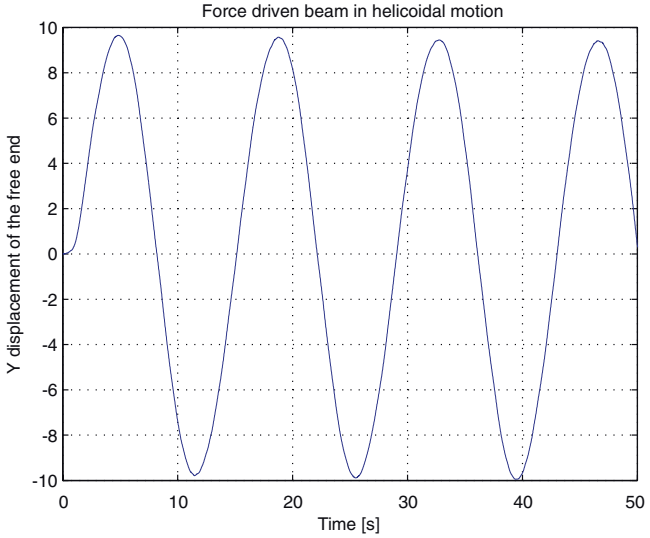

Fig. 9. Force driven flexible beam in a helicoidal motion: Y-displacement of the free end.

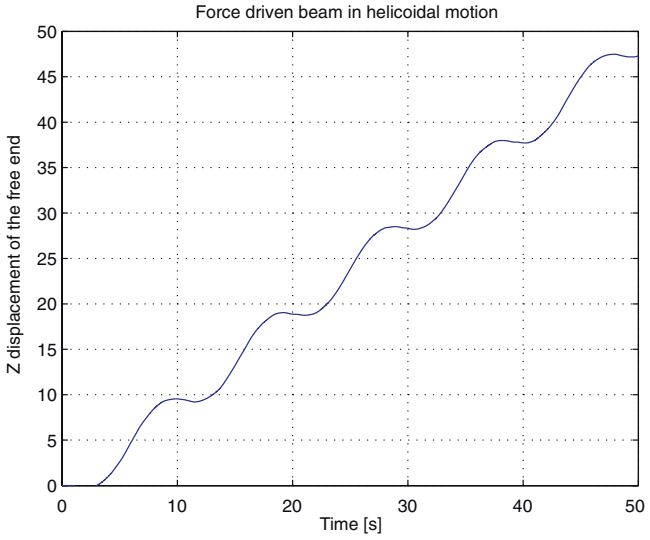

Fig. 10. Force driven flexible beam in a helicoidal motion: Z-displacement of the free end.

a new variable a can be introduced at the contact point, defined as the *approach* (Fig. 12). When inter-penetration occurs we have $a > 0$ and $q < 0$. Without inter-penetration we have that $a = 0$ and $q > 0$. By combining both situations we arrive to the contact condition $q + a \geqslant 0$, which implies $q = -a$ for the case of inter-penetration (for further details see [29,30]). A suitable phenomenological model for the contact forces expressed as a function of the approach between the contact bodies must be introduced, where the magnitude of a will depend on the chosen potential contact model. In this work we will adopt an elastic potential by using a piecewise linear contact force like that plotted in Fig. 13, where the contact stiffness k_s is displayed.

By using again the *discrete directional derivative* concept [23,24], the expression of the elastic forces for the energy

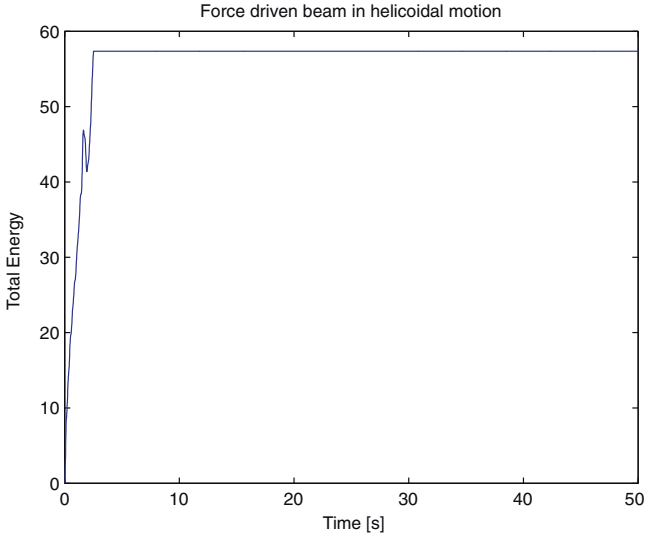

Fig. 11. Force driven flexible beam in a helicoidal motion: total energy of the system.

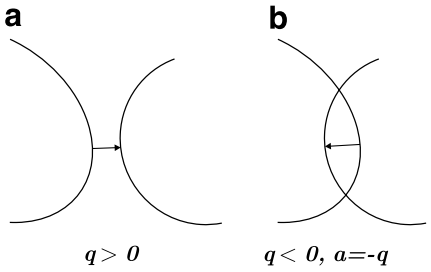

Fig. 12. (a) Non-inter-penetration case: $a = 0$ and $q > 0$ and (b) inter-penetration case: $q = -a$.

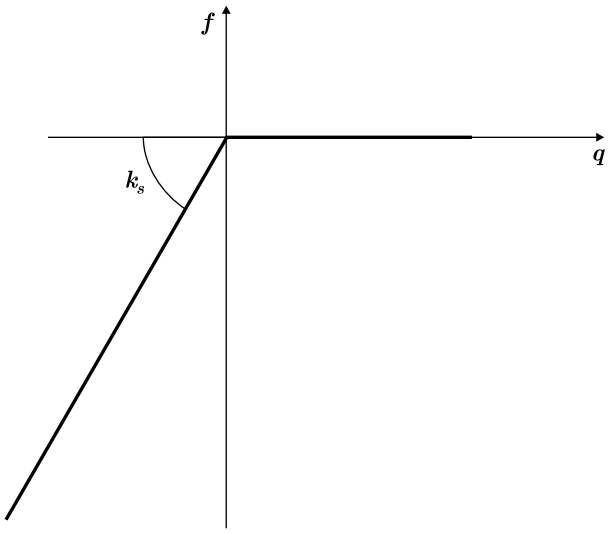

Fig. 13. Elastic potential: piecewise linear contact force.

preserving integration scheme must satisfy the condition established by Eq. (72)

$$(q_{n+1} - q_n)\frac{\partial V}{\partial q}\bigg|^{*}_{n+\frac{1}{2}} = V_{n+1} - V_n \tag{107}$$

where the potential $V(q)$ has for expression

$$V = \int_{q_0}^{q} f(q)\mathrm{d}q + V_0 \tag{108}$$

hence the elastic force expression for the energy preserving scheme writes

$$\left.\frac{\partial V}{\partial q}\right|^{*}_{n+\frac{1}{2}} = \frac{1}{q_{n+1}-q_n}\int_{q_0}^{q_{n+1}} f(q)\mathrm{d}q - \int_{q_0}^{q_n} f(q)\mathrm{d}q = \frac{1}{q_{n+1}-q_n}\int_{q_n}^{q_{n+1}} f(q)\mathrm{d}q \tag{109}$$

By computing the derivative of this expression with respect of $q_{n+\frac{1}{2}}$, we obtain the stiffness contribution as

$$K = \frac{2}{(q_{n+1}-q_n)^2} f(q_{n+1})(q_{n+1}-q_n) - \int_{q_n}^{q_{n+1}} f(q)\mathrm{d}q = \frac{2}{(q_{n+1}-q_n)} f(q_{n+1}) - \left.\frac{\partial V}{\partial q}\right|^{*}_{n+\frac{1}{2}} \tag{110}$$

4.3.2. Impact of a physical pendulum on a rigid stop

This example deals with the impact of a physical pendulum on a rigid stop. The pendulum is 1 m long and is subjected to the action of the gravitational field. The beam properties are: cross-section area $A = 0.0005\ \mathrm{m}^2$, section inertias $I_x = 2\times10^{-7}\ \mathrm{m}^4$ and $I_y = I_z = 1\times10^{-7}\ \mathrm{m}^4$, elastic modulus $E = 2.1\times10^{11}\ \mathrm{N/m}^2$, mass density $\rho = 7800\ \mathrm{kg/m}^3$ and Poisson modulus $v = 0.3$. The pendulum was modelled using 10 beam elements. Fig. 14 shows an schematic draw of the model. The initial condition is depicted in the figure, i.e. the pendulum is dropped from its horizontal position with zero initial velocity.

Several tests were performed for different time step sizes and for different values of the contact stiffness k_s. Figs. 15–18 show the time responses of x and y displacements of the tip of the beam and energies for a contact value of $k_s = 1\times10^8$ N/m (the highest value of contact stiffness used in all tests) while Figs. 19–22 are the plots for $k_s = 1\times10^5$ N/m (the lowest contact value).

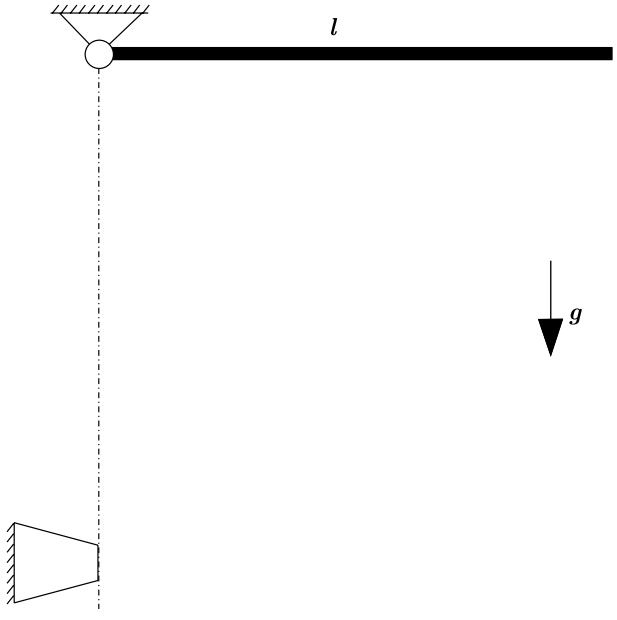

Fig. 14. Impact of a flexible physical pendulum on a rigid stop.

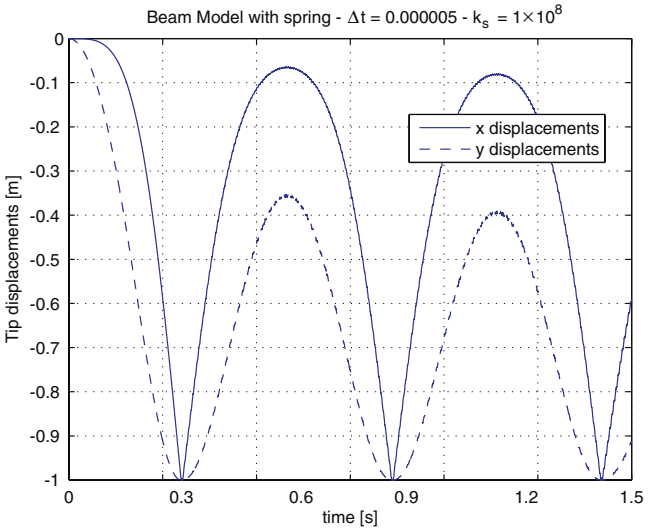

Fig. 15. Impact of a flexible physical pendulum on a rigid stop: x- and y-displacements for the flexible model of impact with $k_s = 1\times10^8$ N/m.

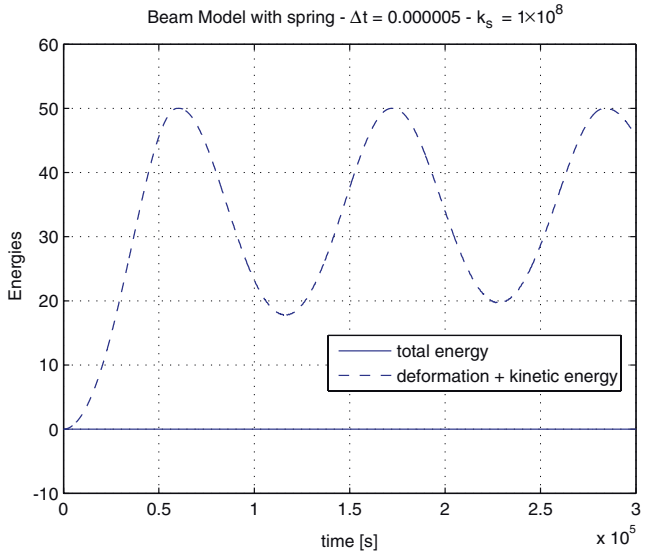

Fig. 16. Impact of a flexible physical pendulum on a rigid stop: energy preserving for the flexible impact model with $k_s = 1\times10^8$ N/m.

Very rapid vibration oscillations are excited in the beam after the first impact, specially for higher values of the contact coefficient k_s, as it can be seen in Figs. 17 and 18. For this reason, the tip of the beam is rapidly oscillating at the time of approaching the stop at second impact, and the computation of motion after impact may present very different responses.

Fig. 23 shows the convergence study for different values of the coefficient k_s. The error is measured as

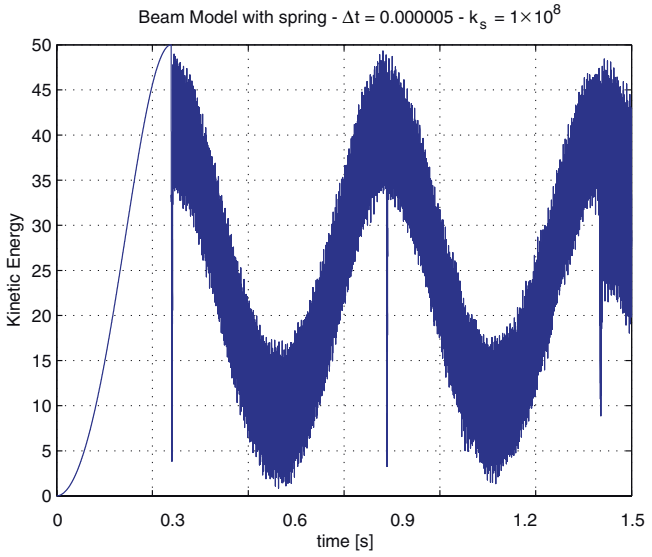

Fig. 17. Impact of a flexible physical pendulum on a rigid stop: kinetic energy for the flexible impact model, with $k_s = 1 \times 10^8$ N/m.

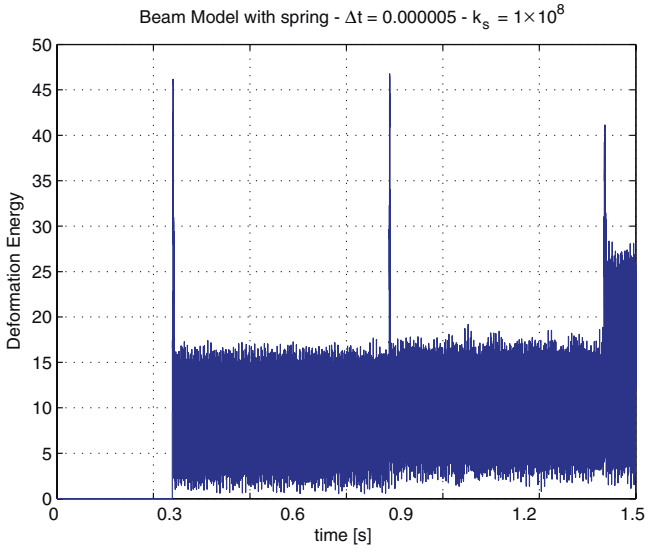

Fig. 18. Impact of a flexible physical pendulum on a rigid stop: deformation energy for the flexible impact model, with $k_s = 1 \times 10^8$ N/m.

$$\epsilon = \sqrt{\sum_{t=t_i}^{t=t_f} [u_1(t) - u_2(t)]^2} \tag{111}$$

considering u_1 as the exact solution, computed with the smallest time step size used in computations. The sample times are chosen at 1.00 s, 1.01 s, 1.02 s, 1.03 s, 1.04 s and 1.05 s. It can be seen that for decreasing k_s, the accuracy grows. The integration scheme verifies first order accuracy, although it is usually second order accurate for 2D standard problems. This loss of accuracy is caused by the discontinuities introduced by the impact problem.

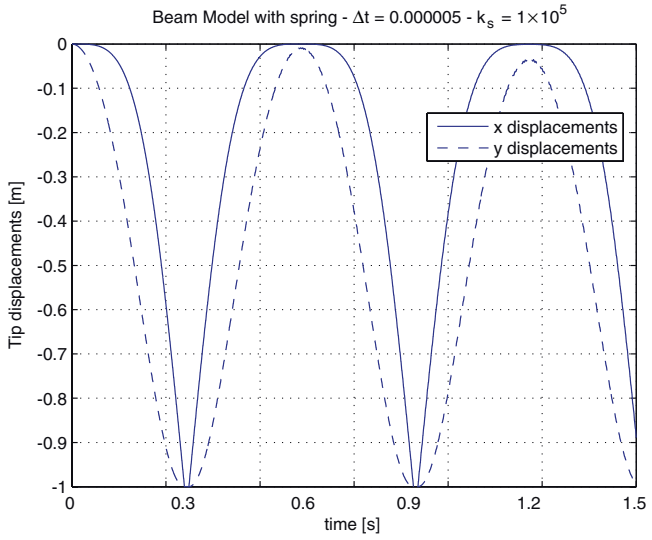

Fig. 19. Impact of a flexible physical pendulum on a rigid stop: x- and y-tip displacements for the flexible impact model with $k_s = 1 \times 10^5$ N/m.

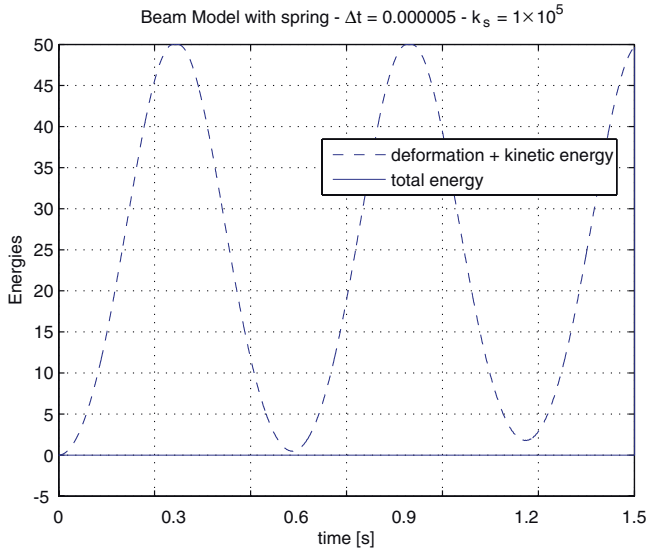

Fig. 20. Impact of a flexible physical pendulum on a rigid stop: energy preserving for the flexible impact model with $k_s = 1 \times 10^5$ N/m.

4.3.3. Oblique impact of an elastic bar against a rigid wall

This example is a modification of that presented in Ref. [31], adding complexity to the model. In that case the flexible bar was modelled using truss-type elements instead of the beam elements of our model, which is then able to account for flexural behaviour.

Fig. 24 sketches the problem. An elastic bar impacts against a vertical rigid wall with an angle of incidence θ and always moves in an horizontal line. The initial configuration is defined by $\theta = 35.2^\circ$ and $v_0 = 2$ m/s. The bar is 1 m long, with a mass $m = 20$ kg and is made of a material with a Young modulus of 1×10^9 N/m^2, Poisson ratio 0.3 and mass density $\rho = 7850$ kg/m^3. The total time integration is 4 s and the contact stiffness is $k_s = 1 \times 10^7$ N/m.

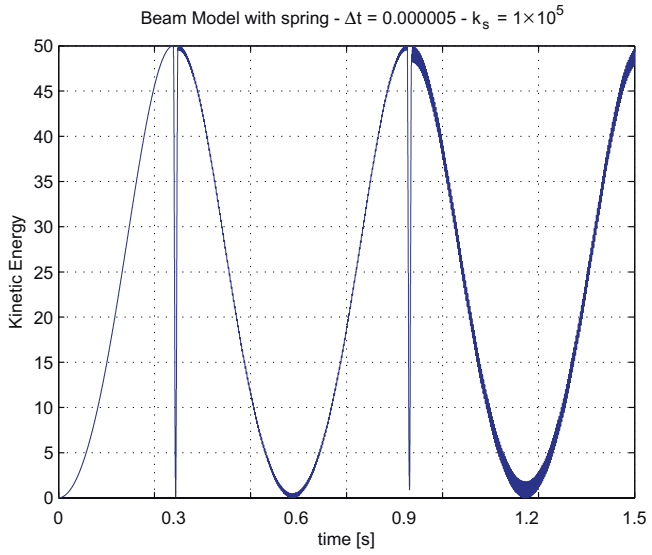

Fig. 21. Impact of a flexible physical pendulum on a rigid stop: kinetic energy for the flexible impact model, with $k_s = 1 \times 10^5$ N/m.

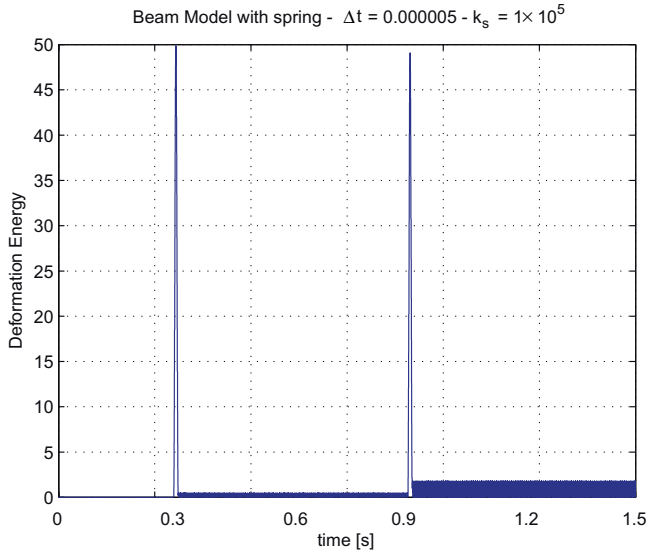

Fig. 22. Impact of a flexible physical pendulum on a rigid stop: deformation energy for the flexible impact model, with $k_s = 1 \times 10^5$ N/m.

The finite elements model consists of 20 beam elements and the time step size adopted is $\Delta t = 1 \times 10^{-4}$ s.

Fig. 25 shows the x-coordinate time evolution of the two edges of the bar. It can be clearly seen the first impact, the subsequent rotation of the bar, the second impact and then the bar bouncing away. Energies are plotted in Fig. 26, where it can be observed that the total energy is exactly conserved.

We remark that our results can be compared with those presented by García Orden and Goicolea [31]. However, we should take into account that in their model they only considered axial deformation effects. Owing to this fact, the responses of the kinetic and deformation energies computed with our beam model differ from theirs.

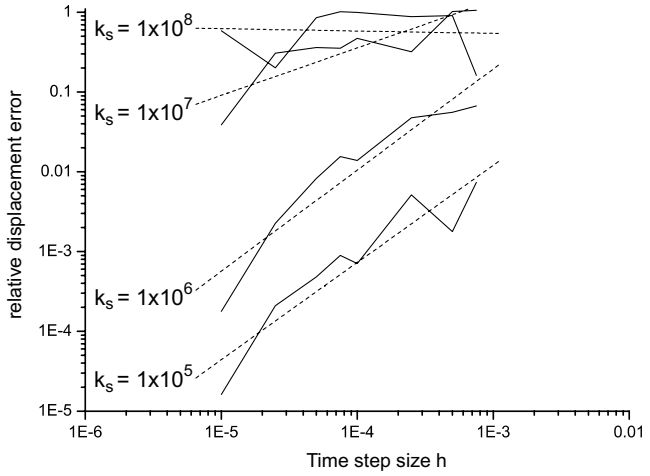

Fig. 23. Impact of a flexible physical pendulum on a rigid stop: convergence study for different values of k_s.

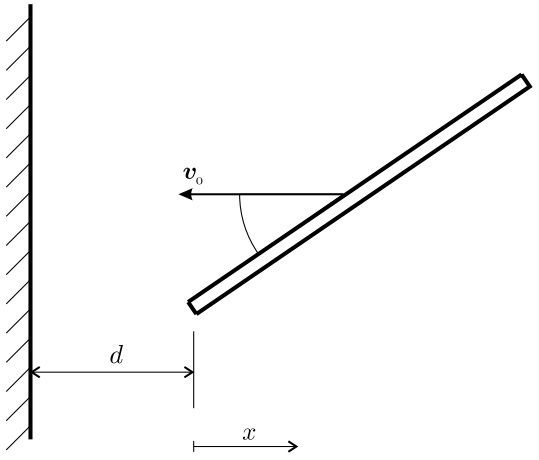

Fig. 24. Flexible beam against rigid wall.

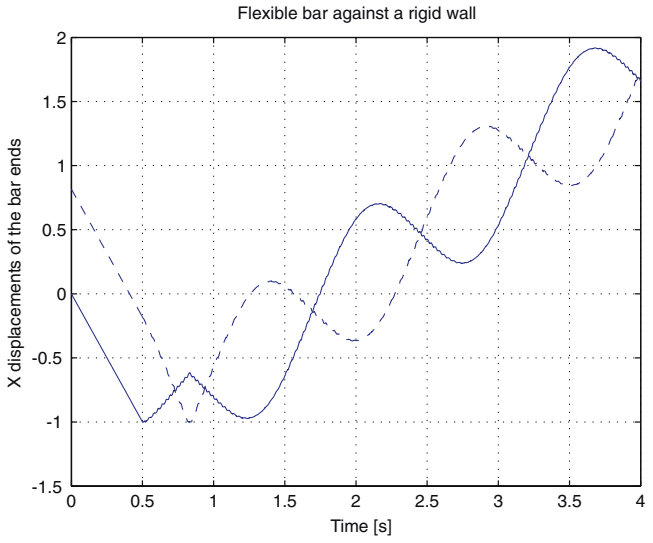

Fig. 25. Flexible beam against rigid wall: time response of the X-coordinate of beam ends.

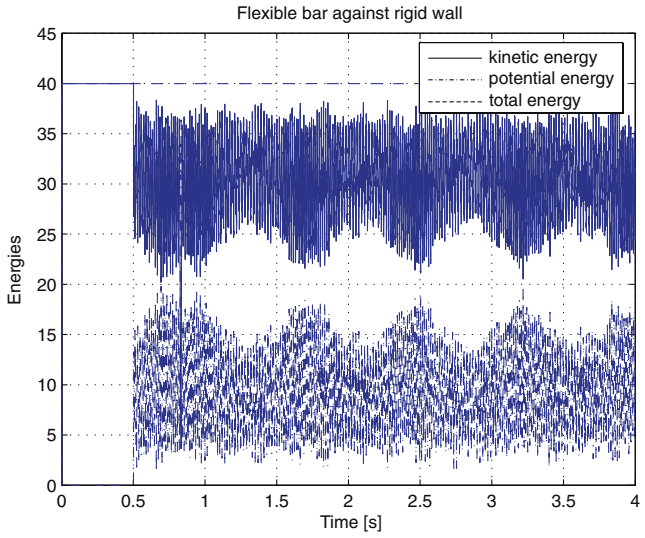

Fig. 26. Flexible beam against rigid wall: kinetic, deformation and total energy.

5. Conclusions

A large rotations nonlinear beam finite element model was developed, in both a classical formulation and an energy conserving formulation. The element makes several simplifications that lead to compact expressions and is simple to be adapted to the energy conserving algorithm.

Full analytical expressions of the internal forces, inertia forces, stiffness and mass matrices are given in the text, allowing the reader to easily implement the element. The intermittent contact problem was also introduced, by using a simple model that relates contact forces with the interpenetration between bodies.

Examples of application to different test cases in 2D and 3D situations have been presented, with comparison of results with those of the literature. The numerical results show the element is able to handle large displacements and rotations under hypothesis of small strains, with an excellent agreement between the obtained results and those found in literature. The formulation presented in this work leads to the same convergence rates as reported in bibliography for 3D examples of beams formulated using different time integration schemes with energy preservation [18,13,28,22].

Acknowledgements

This work has received financial support from *Consejo Nacional de Investigaciones Científicas y Técnicas* (*CONICET*), *Agencia Nacional de Promoción Científica y Tecnológica* (*ANPCyT*) and *Universidad Nacional del Litoral* (*UNL*) from Argentina, and from the *European Community* through grant *SYNCOMECS* (SYNthesis of COmpliant MEChanical Systems) project UE FP6-2003-AERO-1-516183.

References

[1] Lens E, Cardona A, Géradin M. Energy preserving time integration for constrained multibody systems. Multibody System Dyn 2004;11:41–61.
[2] Lens E. Energy preserving/decaying time integration schemes for multibody systems dynamics. PhD thesis, Universidad Nacional del Litoral, Argentina; 2006.
[3] Reissner E. On one dimensional large-displacement finite strain beam theory. Stud Appl Math 1973;52:87–95.
[4] Bathe KL, Bolourchi S. Large displacement analysis of three-dimensional beam structures. Int J Numer Methods Eng 1979;14:961–86.
[5] Simo J. A finite strain beam formulation. Part 1. Comput Methods Appl Mech Eng 1985;49:53–70.
[6] Cardona A, Géradin M. A beam finite element non-linear theory with finite rotations. Int J Numer Methods Eng 1988;26:2403–38.
[7] Hughes T. Analysis of transient algorithms with particular reference to stability behaviour. In: Belytschko T, Hughes T, editors. Computational methods for transient analysis. North Holland; 1983.
[8] Bauchau O. Computational schemes for flexible, non-linear multibody systems. Multibody System Dyn 1998;2:169–225.
[9] Ibrahimbegovic A, Mamouri S, Taylor R, Chen J. Finite element method in dynamics of flexible multibody systems: modelling of holonomic constraints and energy conserving integration schemes. Multibody System Dyn 2000;4:195–223.
[10] Love E. A treatise of the mathematical theory of elasticity. Dover; 1940.
[11] Ibrahimbegovic A. On finite element implementation of geometrically nonlinear Reissner's beam theory: three dimensional curved beam. Comput Methods Appl Mech Eng 1995;112:49–71.
[12] Romero I, Armero F. An objective finite element approximation of the kinematics of geometrically exact rods and its use in the formulation of an energy–momentum conserving scheme in dynamics. Int J Numer Methods Eng 2002;54:1683–716.
[13] Bottasso CL, Borri M. Energy preserving/decaying schemes for nonlinear beam dynamics using the helicoidal approximation. Comput Methods Appl Mech Eng 1997;143:393–415.
[14] Bottasso C, Borri M. Integrating finite rotations. Comput Methods Appl Mech Eng 1998;164:307–31.
[15] Borri M, Bottasso C, Trainelli L. Integration of elastic multibody systems by invariant conserving/dissipating algorithms. I. Formulation. Comput Methods Appl Mech Eng 2001;190:3669–99.
[16] Bottasso C, Borri M, Trainelli L. Integration of elastic multibody systems by invariant conserving/dissipative algorithms. II. numerical schemes and applications. Comput Methods Appl Mech Eng 2001;190:3701–33.
[17] Borri M, Bottasso C, Trainelli L. An invariant-preserving approach to robust finite-element multibody simulation. Z Angew Math Mech (ZAMM) 2003;83(10):663–76.
[18] Leyendecker S, Betsch P, Steinmann P. Objective energy–momentum conserving integration for the constrained dynamics of geometrically exact beams. Comput Methods Appl Mech Eng 2006;195:2313–33.
[19] Betsch P, Steinmann P. Frame-indifferent beam finite elements based upon the geometrically exact beam theory. Int J Numer Methods Eng 2002;54:1775–88.
[20] Betsch P, Steinmann P. Constrained dynamics of geometrically exact beams. Comput Mech 2003;31:49–59.
[21] Bathe KJ. Conserving energy and momentum in nonlinear dynamics: a simple implicit time integration scheme. Comput Struct 2007;85:437–45.
[22] Géradin M, Cardona A. Flexible multibody dynamics: a finite element approach. John Wiley & Sons Ltd.; 2000.
[23] Gonzalez O. Mechanical systems subject to holonomic constraints: differential–algebraic formulations and conservative integration. Physica D 1999;132:165–74.
[24] Gonzalez O. Time integration and discrete hamiltonian systems. J Nonlinear Sci 1996;6:449–67.

[25] Cardona A, Géradin M. Time integration of the equations of motion in mechanism analysis. Comput Struct 1989;33:801–20.
[26] Simo JC, Vu-Quoc L. On the dynamics in space of rods undergoing large motions. A geometrically exact approach. Comput Methods Appl Mech Eng 1988;66:125–61.
[27] Ibrahimbegovic A, Mikdad MA. Finite rotations in dynamics of beams and implicit time-stepping schemes. Int J Numer Methods Eng 1998;41:781–814.
[28] Cardona A. An integrated approach to mechanism analysis, PhD thesis. Faculté des Sciences Appliquées, Université of Liège, Belgique, 1989.
[29] Bottasso CL, Trainelli L. Implementation of effective procedures for unilateral contact modelling in multibody dynamics. Mech Res Commun 2001;28(3):233–46.
[30] Bauchau O. Analysis of flexible multibody systems with intermittent contacts. Multibody System Dyn 2000;4:23–54.
[31] García Orden JC, Goicolea J. Conserving properties in constrained dynamics of flexible multibody systems. Multibody System Dyn 2000;4:225–44.